# I-35/SH-7 Subsurface Investigation

## FINAL REPORT

ODOT TASK ORDER NUMBER 2160-20-06

**Submitted to:**
Office of Research and Implementation
Oklahoma Department of Transportation

**Submitted by:**
Matias M. Mendez Larrain
Syed Ashik Ali
Kenneth R. Hobson
Tom Scullion*
Musharraf Zaman

School of Civil Engineering and Environmental Science (CEES)
The University of Oklahoma
*Texas Transportation Institute, Texas A&M University


December 2021

# SI* (MODERN METRIC) CONVERSION FACTORS

## APPROXIMATE CONVERSIONS TO SI UNITS

| SYMBOL | WHEN YOU KNOW | MULTIPLY BY | TO FIND | SYMBOL |
|---|---|---|---|---|
| | | **LENGTH** | | |
| in | inches | 25.4 | millimeters | mm |
| ft | feet | 0.305 | meters | m |
| yd | yards | 0.914 | meters | m |
| mi | miles | 1.61 | kilometers | km |
| | | **AREA** | | |
| $in^2$ | square inches | 645.2 | square millimeters | $mm^2$ |
| $ft^2$ | square feet | 0.093 | square meters | $m^2$ |
| $yd^2$ | square yard | 0.836 | square meters | $m^2$ |
| ac | acres | 0.405 | hectares | Ha |
| $mi^2$ | square miles | 2.59 | square kilometers | $km^2$ |
| | | **VOLUME** | | |
| fl oz | fluid ounces | 29.57 | milliliters | mL |
| gal | gallons | 3.785 | liters | L |
| $ft^3$ | cubic feet | 0.028 | cubic meters | $m^3$ |
| $yd^3$ | cubic yards | 0.765 | cubic meters | $m^3$ |
| | | NOTE: volumes greater than 1000 L shall be shown in $m^3$ | | |
| | | **MASS** | | |
| oz | ounces | 28.35 | grams | g |
| lb | pounds | 0.454 | kilograms | kg |
| T | short tons (2000 lb) | 0.907 | megagrams (or "metric ton") | Mg (or "t") |
| | | **TEMPERATURE (exact degrees)** | | |
| $^oF$ | Fahrenheit | 5 (F-32)/9<br>or (F-32)/1.8 | Celsius | $^oC$ |
| | | **ILLUMINATION** | | |
| fc | foot-candles | 10.76 | lux | Lx |
| fl | foot-Lamberts | 3.426 | candela/$m^2$ | $cd/m^2$ |
| | | **FORCE and PRESSURE or STRESS** | | |
| lbf | poundforce | 4.45 | newtons | N |
| $lbf/in^2$ | poundforce per square inch | 6.89 | kilopascals | kPa |

## APPROXIMATE CONVERSIONS FROM SI UNITS

| SYMBOL | WHEN YOU KNOW | MULTIPLY BY | TO FIND | SYMBOL |
|---|---|---|---|---|
| | | **LENGTH** | | |
| mm | millimeters | 0.039 | inches | in |
| m | meters | 3.28 | feet | ft |
| m | meters | 1.09 | yards | yd |
| km | kilometers | 0.621 | miles | mi |
| | | **AREA** | | |
| $mm^2$ | square millimeters | 0.0016 | square inches | $in^2$ |
| $m^2$ | square meters | 10.764 | square feet | $ft^2$ |
| $m^2$ | square meters | 1.195 | square yards | $yd^2$ |
| ha | hectares | 2.47 | acres | Ac |
| $km^2$ | square kilometers | 0.386 | square miles | $mi^2$ |
| | | **VOLUME** | | |
| mL | milliliters | 0.034 | fluid ounces | fl oz |
| L | liters | 0.264 | gallons | Gal |
| $m^3$ | cubic meters | 35.314 | cubic feet | $ft^3$ |
| $m^3$ | cubic meters | 1.307 | cubic yards | $yd^3$ |
| | | **MASS** | | |
| g | grams | 0.035 | ounces | Oz |
| kg | kilograms | 2.202 | pounds | Lb |
| Mg (or "t") | megagrams (or "metric ton") | 1.103 | short tons (2000 lb) | T |
| | | **TEMPERATURE (exact degrees)** | | |
| $^oC$ | Celsius | 1.8C+32 | Fahrenheit | $^oF$ |
| | | **ILLUMINATION** | | |
| lx | lux | 0.0929 | foot-candles | Fc |
| $cd/m^2$ | candela/$m^2$ | 0.2919 | foot-Lamberts | Fl |
| | | **FORCE and PRESSURE or STRESS** | | |
| N | newtons | 0.225 | poundforce | lbf |
| kPa | kilopascals | 0.145 | poundforce per square inch | $lbf/in^2$ |

*SI is the symbol for the International System of Units. Appropriate rounding should be made to comply with Section 4 of ASTM E380.
(Revised March 2003)

## TABLE OF CONTENTS

## LIST OF TABLES

## LIST OF FIGURES

## EXECUTIVE SUMMARY

Reflection cracking, edge cracking, rut and longitudinal edge depressions are some of the major problems in asphalt pavements near the intersection of I-35 and SH-7 in Oklahoma. Specifically, reflection cracking and edge cracking were observed on I-35 from Mile Post 45 to Mile Post 59.5, and severe rut and longitudinal joint depressions were observed on SH-7 located approximately 6 miles west of I-35 heading east approximately 5 miles. The purpose of this Task Order was to perform a subsurface investigation using the Ground Penetrating Radar (GPR) system from Texas Transportation Institute (TTI) to identify locations of subsurface distresses and develop data-driven recommendations for maintenance and rehabilitation. Field testing, namely Fast Falling Weight Deflectometer (FFWD) test and laboratory performance tests on asphalt cores, namely Semi-Circular Bend (SCB) test, Texas Overlay (OT) test, Tensile Strength Ratio (TSR) test, Indirect Tensile Asphalt Cracking (IDEAL-CT) test and Hamburg Wheel Tracking (HWT) test, were conducted. Finally, Traffic Speed Deflection Device (TSDD) data, collected on the same segments of I-35 and SH-7 by ODOT as part of a pooled fund study conducted by Virginia Tech Transportation Institute (VTTI), were compared with the FFWD data. The key findings of this Task Order are summarized below:

1. The GPR images showed two different types of pavements in the studied section of I-35, namely Jointed Concrete Pavement (JCP) and Continuously Reinforced Concrete Pavement (CRCP). The JCP section showed severe reflection cracking. Excessive truck loading and change in pavement section between shoulders and driving lanes are likely causes of edge failures.
2. Overall, good modulus (E) values were observed on I-35 and low modulus values were observed on the east-bound inside lane of SH-7, where major depressions and ruts were observed.
3. Performance tests were conducted on asphalt cores collected from I-35. None of these tests met the minimum passing criteria for cracking indicating that the studied section on I-35 is prone to further cracking without appropriate maintenance or rehabilitation measures.
4. The HWT tests showed excessive rut in the east-bound and west-bound lanes of SH-7 indicating potential for rut failure. Significantly high rut and roughness were observed on the east-bound inside lane of SH-7 from TSDD measurement.

5. The FFWD and TSDD deflection data under the center of the loads (W1 and D0, respectively) exhibited a correlation of 0.45. The overall $R^2$ between W1 and D0 deflections for both sections were found as 0.21.
6. Based on the LCCA results, the repair/rehabilitation options (from least costly to most costly) were found as follows:
    a. North-bound I-35, north of Mile Post 51.5, outside lane
        i. Cold mill up to 1-in. of the existing pavement and replace with 1.25-in. of BX (PG 64E-28) and 1-in of Crack Attenuating Mix (CAM) (PG 64-28)
    b. I-35 overlay
        i. Place 1.25-in. of BX (PG 64E-28) on top of the existing pavement
    c. East-bound SH-7 inside lane repair options are similar to those recommended in ODOT Task Order 2160-18-09.
        i. Cold mill up to 2-in. of existing pavement and replace with 2-in. of Stone Matrix Asphalt (SMA) (PG 64E-28), or
        ii. Cold mill up to 2-in. of the existing pavement and replace with 2-in. of S4 (PG 64E-28)
    d. SH-7 overlay
        i. Place 0.75-in. of Ultra-Thin Bonded Wearing Course (UTBWC) Type C, or
        ii. Place 1.25-in. of BX (PG 64E-28) on top of the existing section
7. Among the options listed in the LCCA section, using a Permeable Friction Coarse (PFC) mix can address drainage issues like hydroplaning and rooster-tail effects. The Stone Matrix Asphalt (SMA) is a standard mix choice for a balanced mix design (BMD). Using this mix will enhance ODOT's goal of broader implementation of BMD in Oklahoma.
8. Specialized GPR used in this project, in collaboration with TTI/TAMU, collected data at highway speed. This can be a useful tool for selective data-driven coring of pavement, which is a destructive process, for project-level decisions.
9. FFWD or FWD when used in conjunction with TSDD can be a useful tool for validating TSDD results and identifying pavement conditions (project level) confidently. Also, using pavement layer thicknesses from the GPR data at highway speed enhances the utility of TSDD data for network-level application.

# 1. INTRODUCTION

Pavement distresses were observed in a 14.5-mile section of Interstate 35 (I-35) and a 5-mile section of State Highway 7 (SH-7) in Oklahoma. Specifically, raveling, reflection cracking, longitudinal edge cracking and edge failure were observed on the I-35 section beginning at the Carter/Murray county line (Mile Post 45) and extending north to Mile Post 59.5. Figure 1.1 shows longitudinal edge cracking south of Mile Post 52 on I-35. Figure 1.2 shows a photographic view of the distresses observed on I-35 including reflection cracking and crack sealing.

Figure 1.1 Longitudinal edge cracking observed on I-35

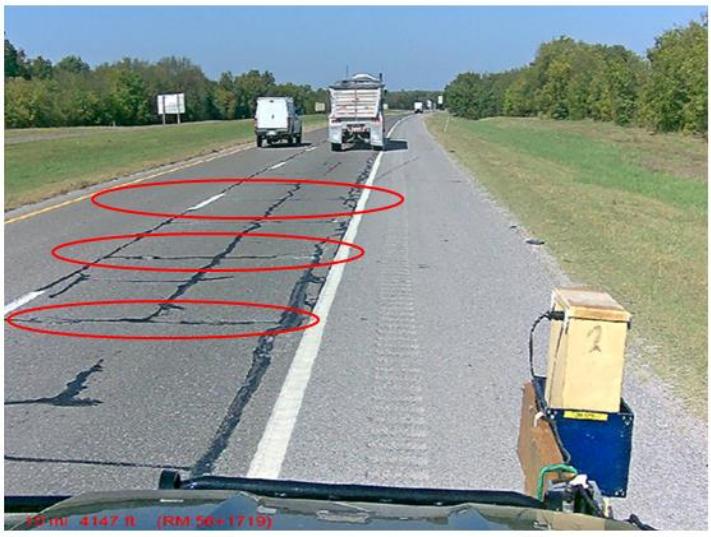

Figure 1.2 Reflective cracking observed on I-35

Longitudinal depressions in the form of rut near the centerline were observed on the SH-7 section located approximately 6 miles west of I-35 heading east approximately 5 miles in Garvin county (ODOT District 7). Figure 1.3 shows a photographic view of the excessive rut observed on SH-7. Figure 1.4 shows a loose or delaminated fabric layer not attached to the pavement below, causing shear failure in the upper Hot Mix Asphalt (HMA) layer. It is also a likely cause of rut.

Figure 1.3 Photographic view of rut observed on SH-7

Figure 1.4 Photographic view of delaminated fabric layer on SH-7

In this subsurface investigation, the Ground Penetrating Radar (GPR) system from Texas Transportation Institute (TTI) at Texas A&M University (TAMU) was used to identify locations of subsurface distresses and develop data-driven recommendations for maintenance

and rehabilitation. Field testing, namely Fast Falling Weight Deflectometer (FFWD) and laboratory performance tests on extracted asphalt cores, namely Semi-Circular Bend (SCB) test, Texas Overlay (OT) test, Tensile Strength Ratio (TSR) test, Indirect Tensile Asphalt Cracking (IDEAL-CT) test and Hamburg Wheel Tracking (HWT) test, were conducted. Finally, Traffic Speed Deflection Device (TSDD) data from the same I-35 and SH-7 sections, collected as part of a pooled fund study conducted by Virginia Tech Transportation Institute (VTTI), were used for selective comparison with the FFWD results.

Ground Penetrating Radar (GPR) is a powerful investigation tool that provides a rapid assessment of pavement subsurface conditions at traffic speed. Texas Transportation Institute (TTI) at Texas A&M University (TAMU) developed this subsurface data collection and processing system using a 1-GHz air-coupled GPR (TTI-GPR) (Figures 1.5 (a) and (b)). Subsurface data up to a depth of 24 inches from the surface can be collected at highway speed (60-70 MPH) using this system. The GPR system is coupled with a digital video camera for continuous imaging of the tested section. The video images are processed with the GPR data in an integrated way. The video images are used to identify locations of the surface distresses such as cracking and patching and to extract cores and perform other tests selectively. The TTI-GPR system has been used widely in Texas to determine thicknesses of different layers in flexible pavements, defects in base and asphalt layers, areas of segregation and poor joint density, and delamination and moisture issues.

(a) (b)

Figure 1.5 The TTI-GPR system (a) mounted on operating vehicle; (b) in operation collecting data

As a part of a pooled fund study (Pavement Structural Evaluation with Traffic Speed Deflection Devices (TSDDs); TPF-5(385)), the pavement conditions of both SH-7 and I-35 sections studied in this Task Order were assessed using a TSDD. This equipment is capable of measuring surface deflections at close intervals (50 feet) as well as roughness, texture, and rut. The collected data can be used to estimate structural conditions of the pavement. The objective of the pooled-fund study was to establish a research consortium focused on providing participating agencies guidelines on data collection and use the collected data for network- and project-level pavement management applications. Figure 1.6 shows a photograph of the TSDD used in the pooled fund study. Additional details on TSDD can be found elsewhere [1,2,3,4,5,6].

Figure 1.6 Traffic Speed Deflectometer Device (TSDD) used in the pooled fund study TPF-5(385)

### 1.1 Scope of Work

This Task Order was divided into the following steps: collecting project information, collecting data using the TTI-GPR system, analyzing GPR data and identifying distressesd locations, conducting Fast Falling Weight Deflectometer (FFWD) testing selectively based on the GPR data and visual images from the video camera, field sampling from distressed locations, conducting laboratory testing on core samples, and comparing surface deflections obtained from the FFWD testing with the TSDD data selectively.

A kickoff meeting was held on October 5, 2020 between the OU team and the TTI staff to discuss the extent, history, and conditions of the project and to devise a tentative GPR testing

plan. On October 14, 2020, TTI conducted the GPR testing on both sections of I-35 and SH-7. Based on the analyses of the GPR data, the locations of asphalt coring were determined. Longitudinal edge cracking, edge failure, reflection cracking and some surface and minor cracking were observed on I-35 from the GPR and video images. On SH-7, major rut, open longitudinal joints and cracking in old mats were observed. Eleven (11) cores were extracted from the I-35 section on December 8, 2020. The corresponding number of cores extracted (on the same day) from the SH-7 section was five (5). On December 9, Fast Falling Weight Deflectometer (FFWD) tests were conducted over the studied sections. Laboratory tests, namely Semi-Circular Bend (SCB) test, Texas Overlay (OT) test, Indirect Tensile Strength (ITS) test, Ideal Tensile Asphalt Cracking (IDEAL-CT) test, Hamburg Wheel Tracking (HWT) test and volumetric tests were conducted on the extracted cores. Collection of the TSDD data for the I-35 and SH-7 sections was done earlier in 2020. The survey was part of a pooled fund study involving several states nationwide including ODOT. The TSDD results were shared with the OU team by the pavement management group at ODOT. As noted above, the TSDD results were compared selectively with the FFWD results from this Task Order.

## 2. METHODOLOGY AND FIELD INVESTIGATION

### 2.1 Project Location

As noted earlier, a 14.5-mile section of I-35 beginning at the Carter/Murray county line at Mile Post 45 (34.376384, -97.144182) and extending north to Mile Post 59.5 (34.559871, -97.193138) was selected for this study. The studied section on SH-7 started one (1) mile west of the intersection with I-35 (34.510042, -97.194876) and extended five (5) miles west (34.521343, -97.284874) in Garvin county, in District 7. Figure 2.1 shows the beginning and ending points of the studied sections. Based on the District 7 plans, the 14.5-mile section had several modifications of the pavement over the years. Two different pavement types were observed in the studied I-35 section. The section south of Mile Post 52 consisted of 8 to 10 inches of asphalt and 8 inches of Continuously Reinforced Concrete Pavement (CRCP) over 2 inches of cold milled and replaced by 2 inches of asphalt. The section north of Mile Post 52 consisted of 8 to 10 inches of asphalt and 9 inches of Jointed Concrete Pavement (JCP) over 2 inches of cold milled and replaced by 2 inches of asphalt. Based on the Oklahoma Highway System Data, in 2018, the Annual Average Daily Traffic (AADT) of the I-35 section was between 31,400 and 34,800. Comparatively, the SH-7 section consisted of 17 to 21 inches of asphalt

with fabric at 1.5 inches below the surface. Based on the Oklahoma Highway System Data, the AADT on the SH-7 section was between 3,600 and 6,700 in 2018.

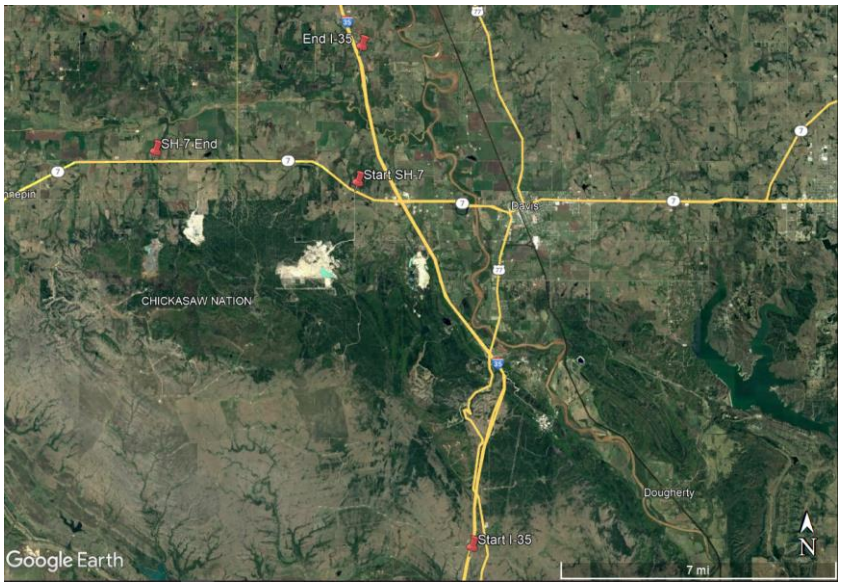


Figure 2.1 Google satellite image of the test section

### 2.2 Ground Penetrating Radar Test and Selection of Core Locations

The subsurface investigation using GPR was performed on the above-mentioned sections of I-35 and SH-7 using the 1-GHz air-coupled TTI-GPR with the help of Dr. Tom Scullion from Texas Transportation Institute (TTI) at Texas A&M University. The east-bound lanes of SH-7 and the north-bound lanes of I-35 were included in this investigation. Multiple runs were performed to identify the pavement conditions. The GPR data was collected at highway speed (60-70 MPH). Therefore, traffic control setup was not needed for this task. The GPR data were collected on Wednesday, October 14, 2020.

The collected GPR data were sorted, filtered, and analyzed using the software developed by TTI. The GPR data were then used to determine the layer thicknesses, presence of moisture, voids, stripping and other anomalies in the asphalt pavement, which could be responsible for the pavement distresses. The GPR results were used to identify areas for extraction of cores. Figure 2.2 shows an example of the GPR results from the north-bound lane of I-35. On Mile Post 51.5, the GPR images showed the end of the Continuously Reinforced Concrete Pavement (CRCP) section and the beginning of the Jointed Concrete Pavement (JCP) section. The GPR images did not detect any presence of reinforced steel anymore, and reflection cracking started to appear in this segment.


Figure 2.2 GPR and video images from north-bound I-35 section near Mile Post 51.5

The main distresses observed south of Mile Post 51.5 (CRCP) were longitudinal edge cracking and edge failure. Also, some surface raveling and edge failure were observed. North of Mile Post 51.5 (JCP), the main distresses observed were reflection cracking and longitudinal edge cracking. The main cause of longitudinal edge failure is the presence of joint between the shoulder and lane inside the stripe paint. The pavement section in this segment consisted of 6 inches of HMA over CRCP. The shoulder section consisted of 6 inches of HMA over sand asphalt. Therefore, truck loads right at the joint or close to the joint are expected to cause higher deflections and failures. Figure 2.3 shows the difference between the lane and shoulder segments and the FFWD deflections.

Figure 2.4 shows the GPR data collected from the east-bound lane of SH-7. As noted above, the GPR data exhibited an increase in moisture over the joint indicating infiltration of water through the longitudinal joint crack.

A total of twenty-six (26) locations were identified as critical after analyzing the GPR data, and a coring plan was advised. Due to issue with traffic control and safety issues, eleven (11) cores from the I-35 section and five (5) cores from the SH-7 section were extracted.


Figure 2.3 Lane and shoulder segments of I-35 near Mile Post 51.5 and extracted cores

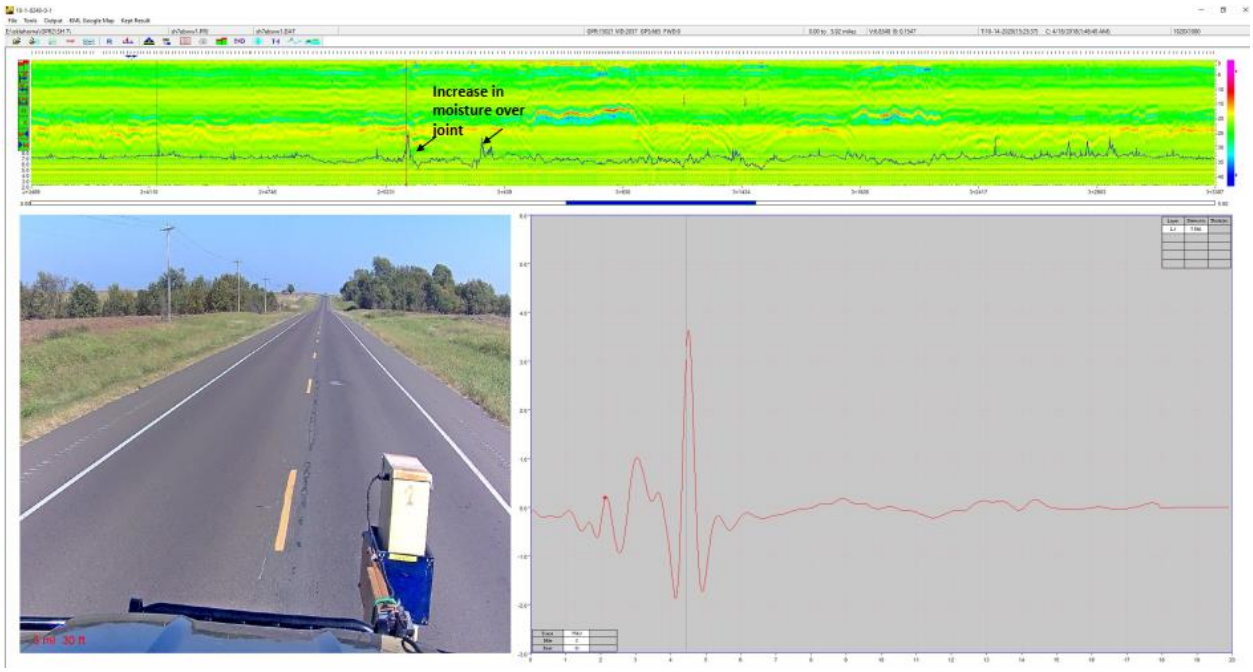


Figure 2.4 GPR and video images from east-bound SH-7 section

### 2.3 Asphalt Coring

Locations of the asphalt cores were established based on the results of the GPR testing. Collection of cores for the study sections was performed on December 8, 2020. District 7 provided traffic control with lane closures and a pilot vehicle. Table 2.1 describes the locations

and notes of the extracted cores. As noted above, sixteen (16) cores were extracted, eleven (11) from the I-35 section and five (5) from the SH-7 section. Figure 2.5 shows a photographic view of the asphalt core extraction. Photographs of the extracted cores from the I-35 and SH-7 sections are included in Appendix A along with notes.

Table 2.1 Locations of the extracted cores

| **Cores I-35** | **Latitude** | **Longitude** | **Direction** | **Core Notes** |
|---|---|---|---|---|
| 2 | 34.46068 | -97.144701 | NB | Mid-lane |
| 3 | 34.46068 | -97.144701 | NB | 2-ft. south of Core 2 |
| 4 | 34.46068 | -97.144701 | NB | Over shoulder, delamination and stripping |
| 5 | 34.468844 | -97.152298 | NB | Mid-lane, thick tack and fabric |
| 6 | 34.468844 | -97.152298 | NB | 2-ft. south of Core 2, fabric |
| 7 | 34.468844 | -97.152298 | NB | Mid. Shoulder, Delamination |
| 8 | 34.477261 | -97.156555 | NB | 1-ft. left of shoulder line, thick tack |
| 12 | 34.550264 | -97.190554 | NB | Mid-lane over crack, filled crack, thick tack and delamination |
| 13 | 34.550264 | -97.190554 | NB | 2-ft. right of shoulder line, crack, delamination, stripping |
| 14 | 34.550264 | -97.190554 | SB | Right wheel path |
| 15 | 34.550264 | -97.190554 | SB | Shoulder line, delamination, stripping and fully cracked bottom layer |
| **Cores SH-7** | **Latitude** | **Longitude** | **Direction** | **Core Notes** |
| 17 | 34.52051 | -97.212729 | WB | Right wheel path through crack, fabric |
| 22 | 34.521305 | -97.237975 | EB | Right wheel path, fabric, delamination, stripping |
| 23 | 34.521305 | -97.237975 | EB | Left wheel path near center line in rutted area, delamination, stripping, cracked |
| 24 | 34.521305 | -97.237975 | WB | Left wheel path over crack, fabric, delamination |
| 25 | 34.521305 | -97.237975 | WB | Right wheel path |

Figure 2.5 Asphalt coring operation on SH-7

### 2.4 Fast Falling Wight Deflectometer Testing

The structural condition assessment of pavement layers plays a critical role in selecting appropriate maintenance and rehabilitation measures by the state transportation agencies. Fast Falling Weight Deflectometer (FFWD) is a deflection-testing device commonly used to determine structural capacity of pavement layers. A Dynatest FFWD equipment with seven geophone sensors (W1 to W7) was used for the FFWD test (Figure 2.6). These tests were conducted at 359 locations on the I-35 and SH-7 sections on December 9, 2020.

Figure 2.6 FFWD test performed on I-35 section at Mile Post 46

The deflection values for the north-bound and south-bound locations on I-35 are shown in Figure 2.7, while deflection values for the east-bound and west-bound locations on SH-7 are shown in Figure 2.8. For safety reasons, FFWD tests were performed only on the right lanes (next to shoulder) in each direction. The deflection values at the center of the FFWD loading plate correspond to W1 sensor, which is an indicator of the overall structural condition of the pavement at the time of testing. The W7 sensor, on the other hand, indicates deflection at a distance of 60 inches from the center of the load, which is an indicator of the subgrade strength.

The air temperature during testing ranged from 31°F to 51°F, as per temperature data collected from the Mesonet site located at Paul's Valley. For the north-bound lane of I-35, FFWD tests were conducted at 124 locations. The highest W1 deflection was recorded as 5.5 mils. From these data, the average deflection was found to be 2.39 mils, with a standard deviation of 0.72 mils. Comparatively, FFWD tests at the south-bound lane of I-35 were conducted at 123 locations. The highest W1 deflection was recorded as 8.19 mils with an average of 2.32 mils and a standard deviation of 0.95 mils. For the east-bound and west-bound lanes of SH-7, a total of 56 locations were tested in each direction. For the east-bound lane, the highest W1 deflection was recorded as 5.2 mils with an average of 3.04 mils and a standard deviation of 0.75 mils. For the west-bound lane, the highest W1 deflection was 4.22 mils with an average of 3.10 mils and a standard deviation of 0.62 mils.

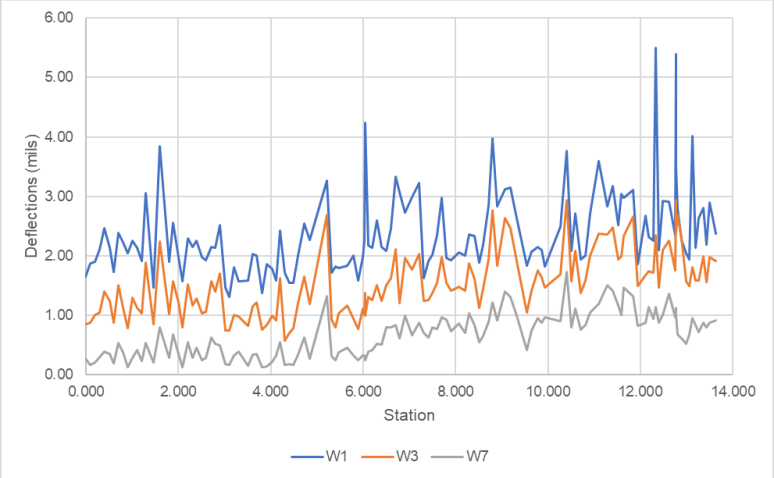


(a)

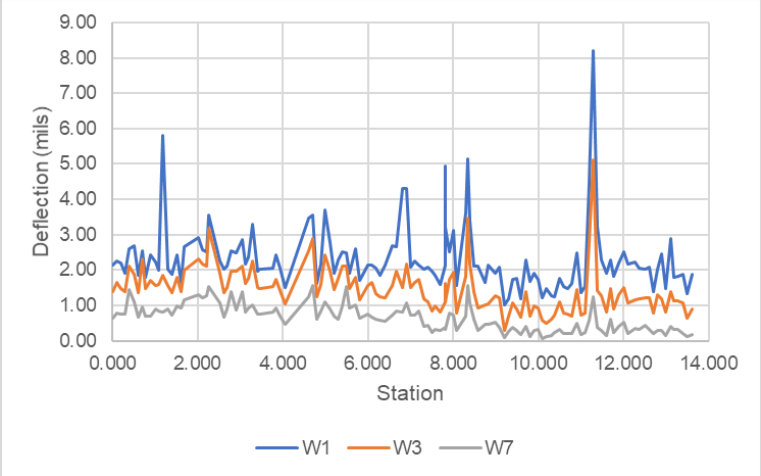


(b)

Figure 2.7 FFWD results for I-35 section: (a) north-bound lane; (b) south-bound lane

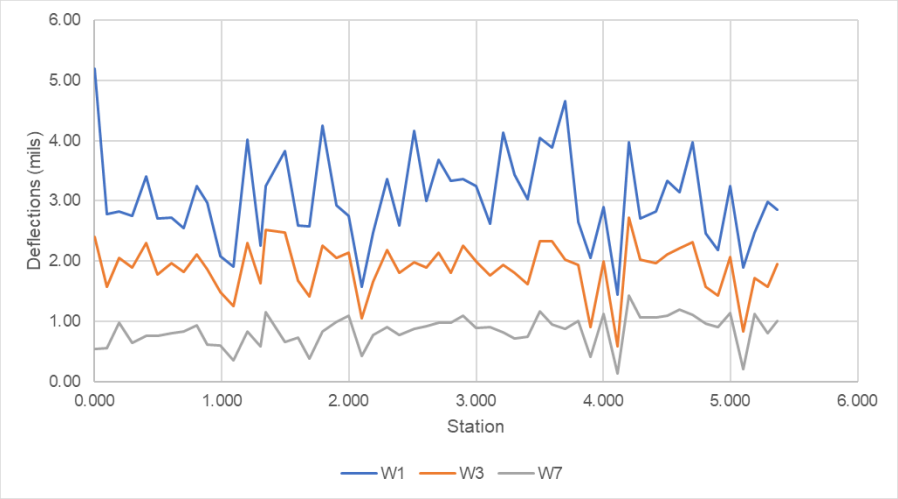


(a)

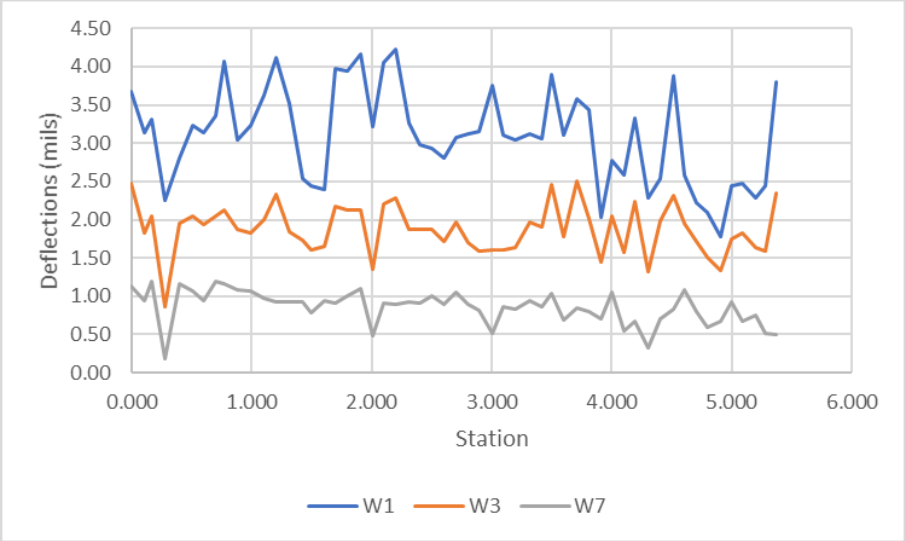


(b)

Figure 2.8 FFWD results for SH-7 section: (a) east-bound lane; (b) west-bound lane

The MODULUS 7.0 program was used to analyze the FFWD data and calculate the normalized maximum deflections of W1 and W7 sensors (with respect to a 9-kip load) and modulus of the pavement layers. Figures 2.9 and 2.10 show the moduli (E) values for surface and subgrade for the I-35 and SH-7 sections, respectively.

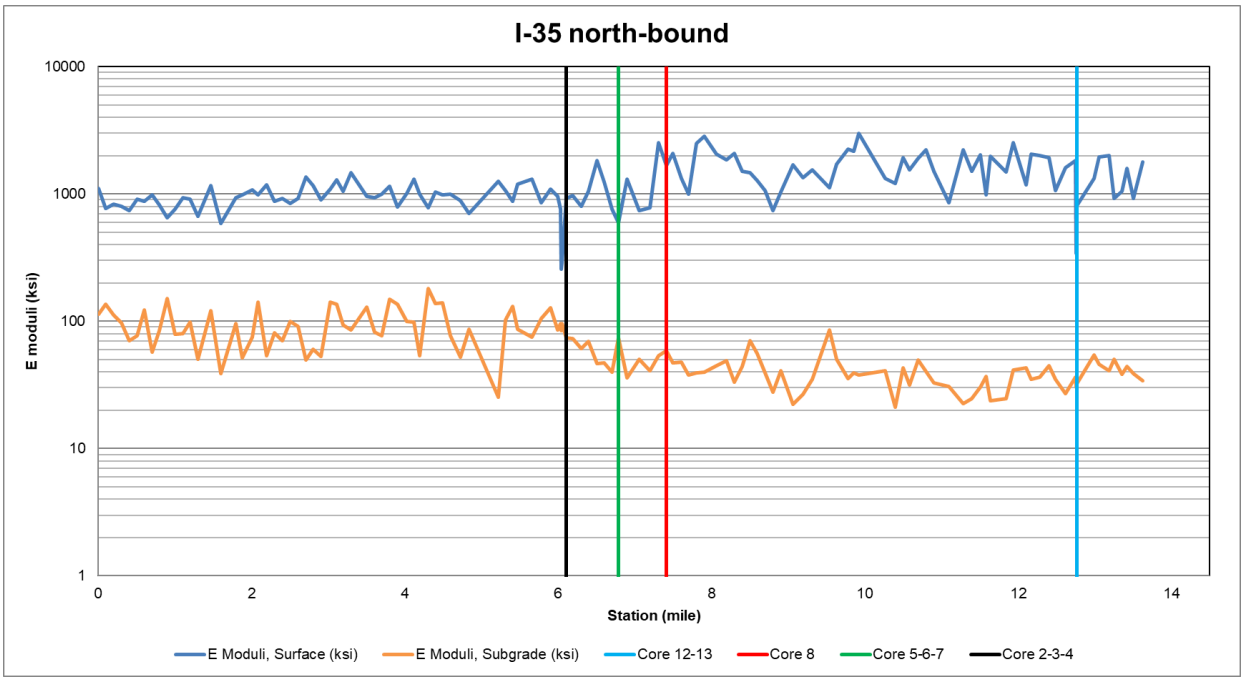


(a)

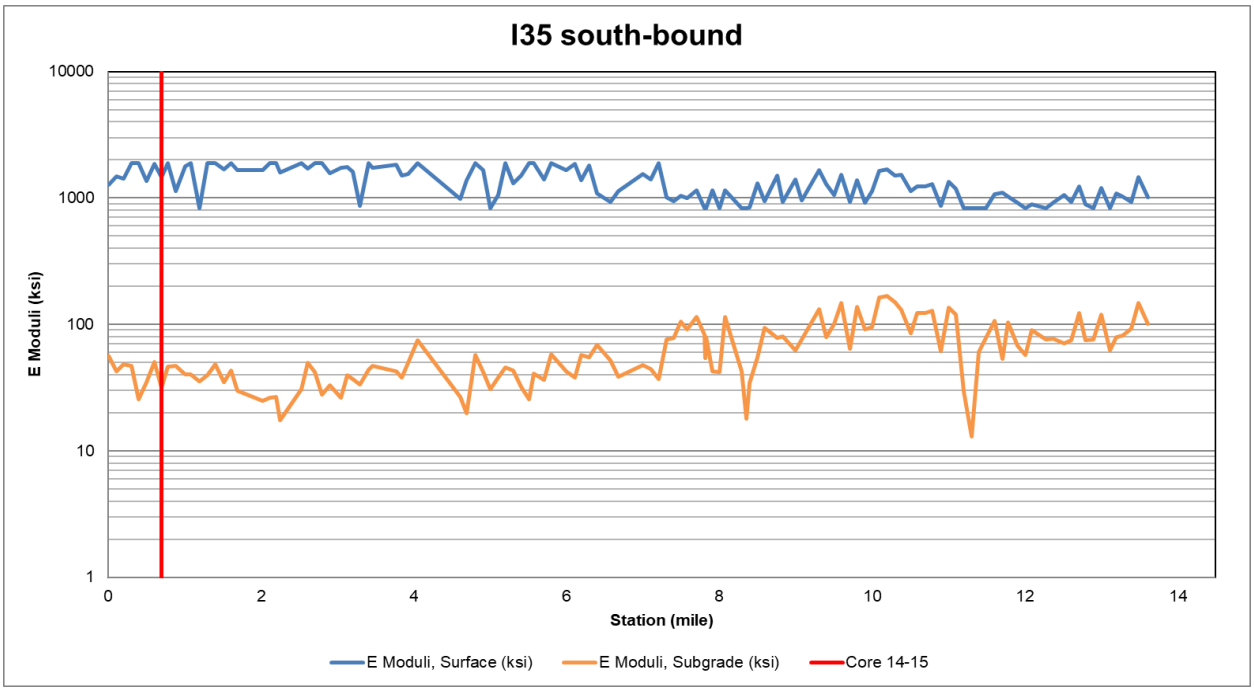


(b)

Figure 2.9 Elastic moduli (E) results for the I-35 section: (a) north-bound; (b) south-bound

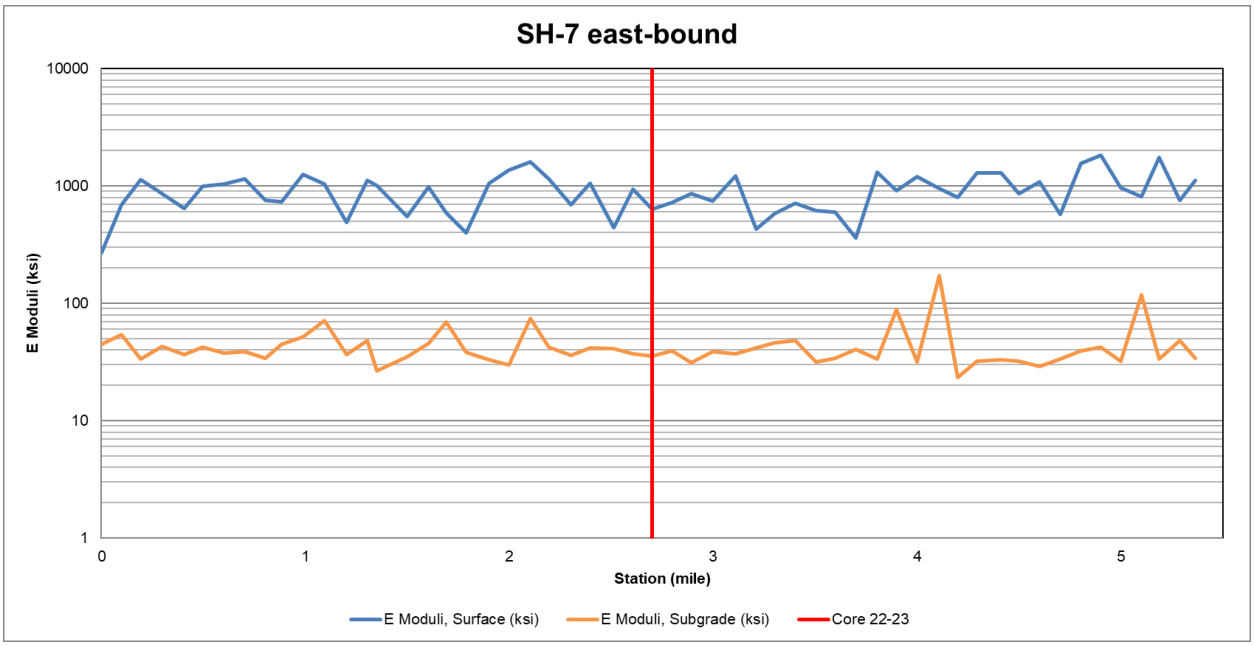


(a)

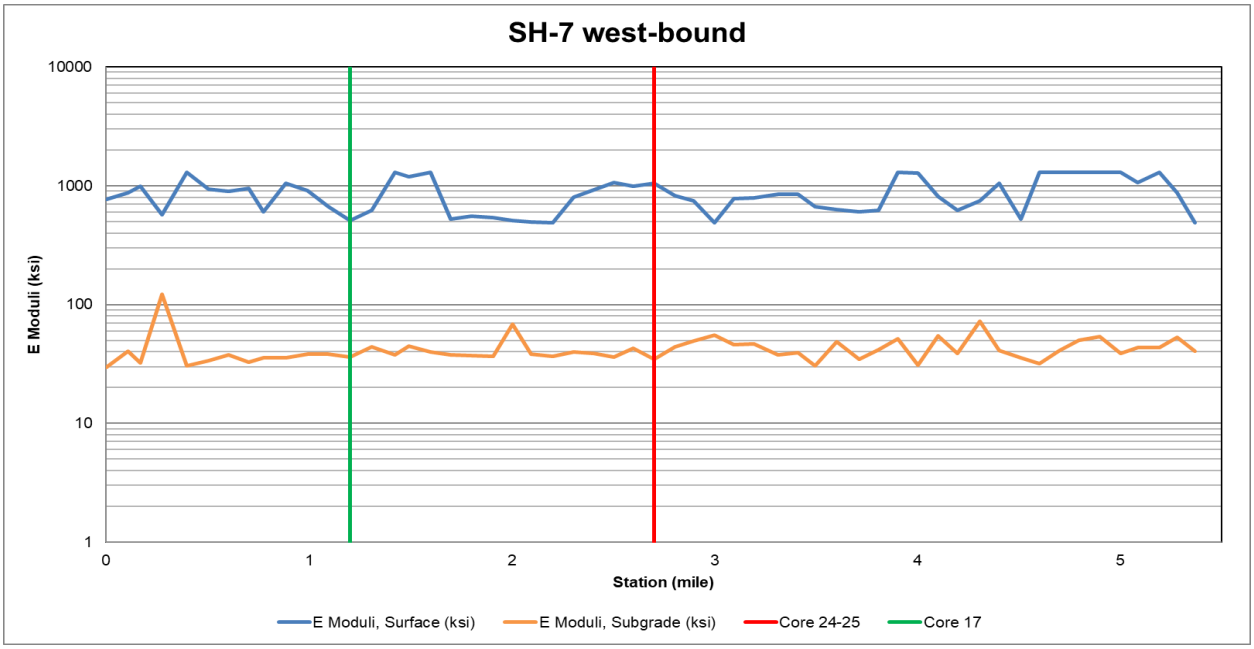


(b)

Figure 2.10 Elastic moduli (E) results for the SH-7 section: (a) east-bound; (b) west-bound

For the surface layer of the east-bound lane of SH-7, the mean and standard deviation of moduli were found as 919.7 and 346.4 ksi, respectively. For the subgrade layer, the corresponding values were found as 44.6 and 23.7 ksi, respectively. For the west-bound lane,

the corresponding mean and standard deviation were 866.6 and 277.7 ksi (for base layer) and 42.7 and 13.8 ksi (for subgrade layer), respectively. From laboratory testing, E values of cores 17, 22-23 and 24-25 were found to be 510, 636 and 1,052 ksi, respectively.

For the I-35 section, the E values were found to be much higher, as expected. The mean and standard deviation were observed as 1,262.2 and 536 ksi, respectively, for the base layer and 66.3 and 35.7 ksi, respectively, for the subgrade in the north-bound lane of I-35. For the south-bound lane, the corresponding mean and standard deviation values were 1,332.2 and 383.2 ksi, respectively, for the surface layer and 65 and 35.3 ksi, respectively, for the subgrade. From laboratory testing, the E moduli of 918, 596, 1,674, 810 and 1,461 ksi were observed for cores 2-3-4, 5-6-7, 8, 12-3, and 14-15, respectively.

## 3. LABORATORY TESTING

Sixteen (16) cores were brought to the OU Broce Laboratory for further testing, eleven (11) cores from the I-35 section and 5 from the SH-7 section. The cores were cleaned and photographed with a ruler next to the core. The digital images of the cores are presented in Appendix A of this report. As noted earlier, the laboratory tests conducted in this project include SCB test, Ideal CT test, Tensile Strength Ratio (TSR) test, HWT test, Texas Overlay test, and volumetric properties of the cores. The results were used to identify the reasons for the observed distresses. Table 3.1 presents the test matrix and the test standards followed in conducting these tests.

Table 3.1 Test performed on the extracted cores

| **Tests on Asphalt Cores** | | |
|---|---|---|
| **Test Name** | **Test Specification** | **Comments** |
| Rice Test | AASHTO T 209 [7] | To determine % density or air void content |
| Density of Asphalt Core | OHD L-14 [8] | Top lift |
| Hamburg Wheel Tracking (HWT) Test | OHD L-55 [9] | Top lift |
| Illinois-Flexibility Index Test (IFIT) | AASHTO TP 124 [10] | Semi-circular specimens of top lift |
| Tensile Strength Ratio (TSR) Test | AASHTO T 283 [11] | Top lift |
| Indirect Tensile Asphalt Cracking Test (IDEAL-CT) | NCHRP Project 195 [12] | Top lift |
| Texas Overlay Test (OT) | Tex-248-F [13] | Top lift |

### 3.1 Density of Extracted Asphalt Cores

Density tests were conducted on the top lifts of the extracted asphalt cores according to OHD L-14 [8]. The maximum theoretical specific gravity (%$G_{mm}$) was determined using the AASHTO T 209 [7] test method for extracted cores from each studied section. Figure 3.1 presents the density values of the extracted cores for the I-35 section. Cores 5 and 6 were given to TTI for their work on this project and were not included in the testing by the OU team. Also, Cores 12 and 13 were cracked. So, they could not be used for density measurements. The average density and standard deviation for the extracted cores from the I-35 section were found to be 92.4% and 0.6%, respectively. Figure 3.2 presents the density values of the extracted cores for the SH-7 section. The average density and standard deviation were found to be 94.9% and 1.2%, respectively. It is likely that these densities were even lower during construction, as traffic-induced compaction increases density to some degree. Lower than required densities can contribute to premature distresses including rut and fatigue cracking.

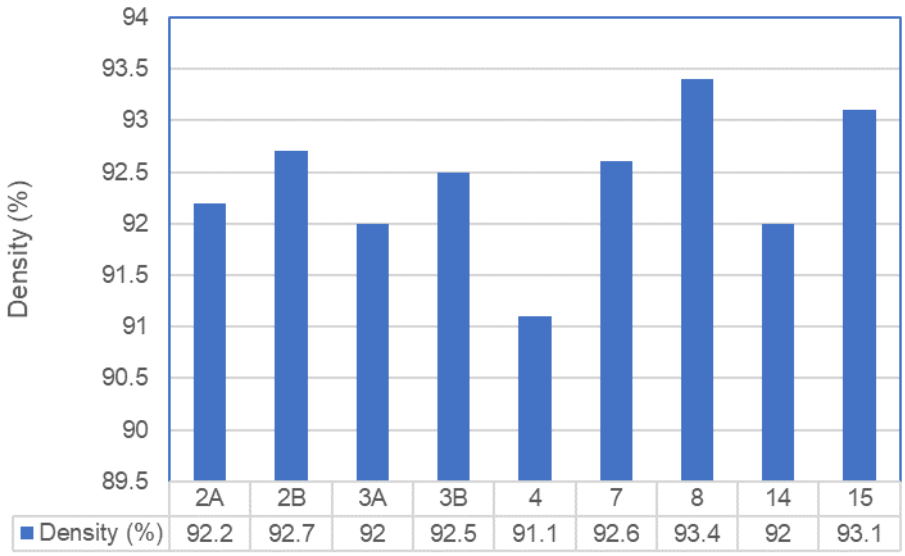


Figure 3.1 Density values of extracted cores from the I-35 section

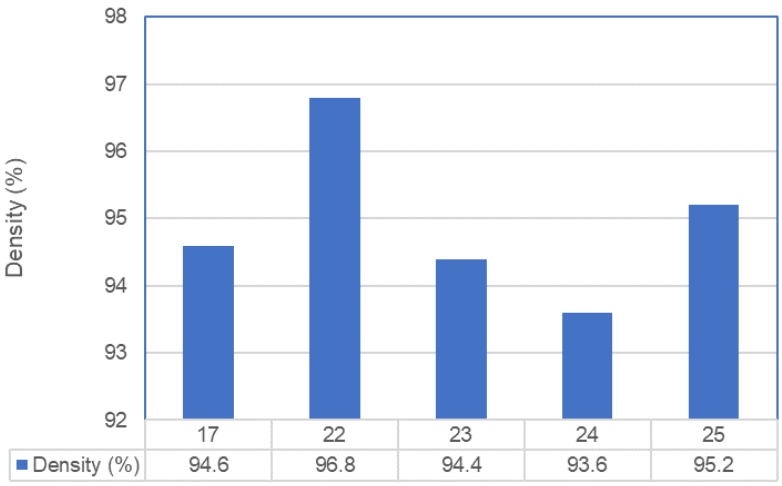


Figure 3.2 Density values of extracted cores from the SH-7 section

### 3.2 Semi-Circular Bend (SCB) Test

Semi-circular Bend tests were conducted on the extracted cores from I-35 to determine their resistance to fatigue cracking. The Illinois-Flexibility Index Test (I-FIT) was conducted in accordance with the AASHTO TP124 [10] method. For this purpose, a 40 mm thick layer was cut out from the top of the core. It was then cut into two semi-circular pieces and a notch of 15 mm depth was cut in each semi-circular piece. The test was conducted by applying a monotonic load at 50 mm/min until failure. The I-FIT test results are presented in Figure 3.3. The Flexibility Index (FI) values were found to be very low for samples 2A, 3A and 3B, and low for sample 2B compared to the acceptable limit (greater than 8). Photographic views of the tested samples are shown in Figure 3.4.

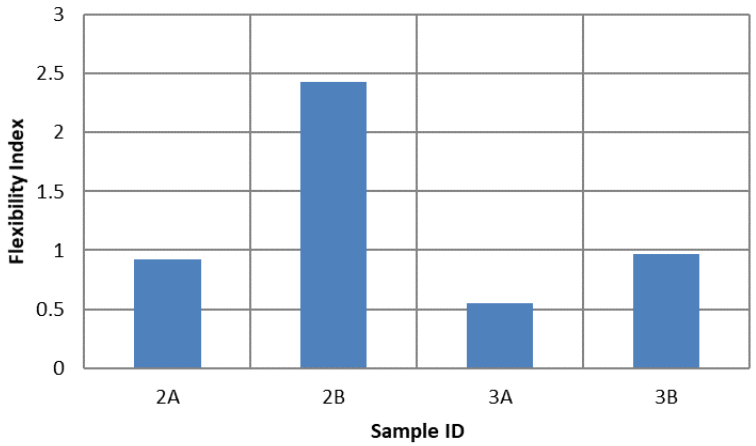


Figure 3.3 I-FIT results for selected cores

(a)

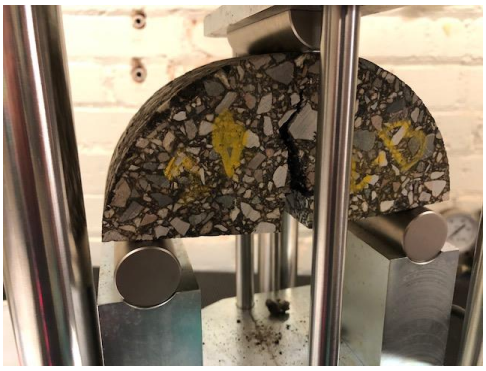

(b)

(c)

(d)

Figure 3.4 Photographic views of tested samples: (a) 2A; (b) 2B; (c) 3A; (d) 3B

### 3.3 Hamburg Wheel Tracking (HWT) Test

Hamburg Wheel Tracking (HWT) tests were conducted on the top lifts of the extracted cores from SH-7 following OHD L-55 [9] to determine their susceptibility to rut and potential for moisture-induced damage. The HWT tests were conducted at 50°C with a wheel pass frequency of 52 passes/minute. The tests were terminated after reaching a maximum rut depth of 20-mm or 20,000-wheel passes, whichever reached first. Figure 3.5 presents the HWT test results for Cores 22/23 and Cores 24/25. Also, Table 3.2 summarizes the results of post-compaction, creep slope and maximum rut depth.

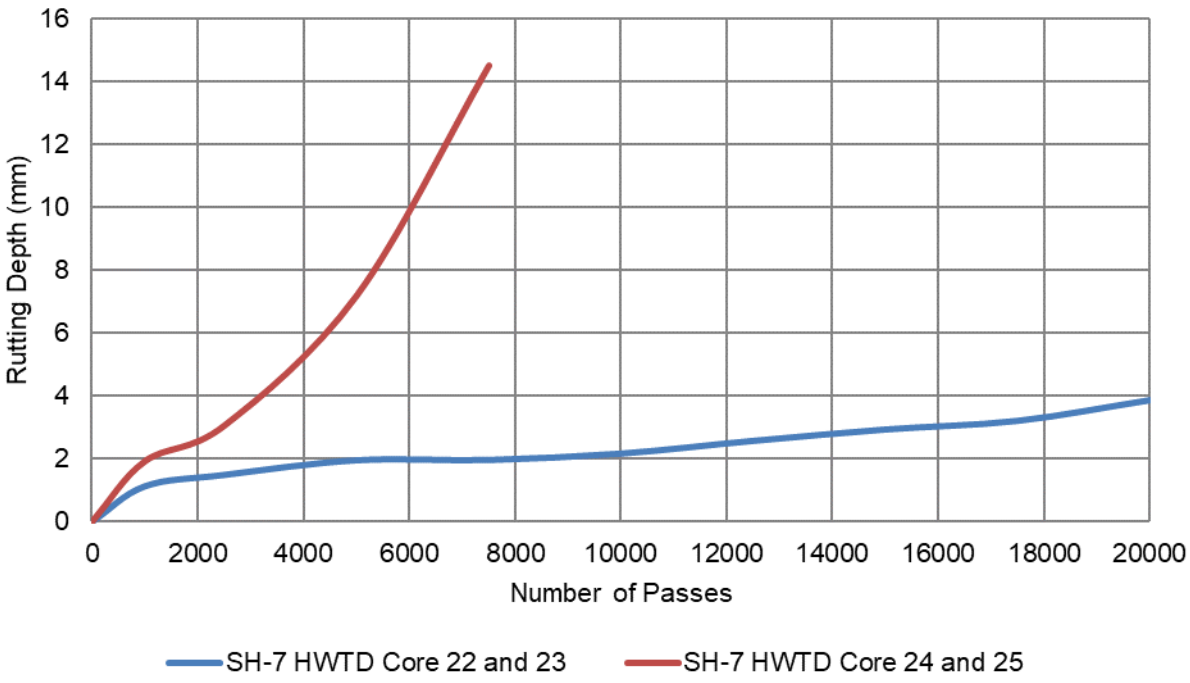


Figure 3.5 The HWT test results for Cores 22/23 and Cores 24/25

Table 3.2 Summary of the HWT results

| Cores | Number of Passes and Rut Depth at Post Compaction | Creep Slope (passes/mm) | Stripping Inflection Point | Maximum Number of Passes | Maximum Rut Depth (mm) |
|---|---|---|---|---|---|
| 22/23 | 1,000 (1.1) | 6,900 | Not Observed | 20,000 | 3.9 |
| 24/25 | 1,000 (2.0) | 1,500 | 2,500 | 7,500 | 14.5 |

The Cores 22/23 performed well in rut and no stripping inflection point was observed (Figure 3.6 (a)). The Cores 24/25, however, did not pass the minimum requirement for rut (<12.5 mm for 20,000 passes). Also, stripping inflection point, which is an indicator of moisture-induced damage, was observed at 2,500 cycles (Figure 3.6 (b)). Figure 3.7 shows delamination of Core 24 (next to longitudinal joint) prior to testing. No other tested cores showed delamination in the top lift.

(a) (b)

Figure 3.6 Photographic views of cores after HWT tests: (a) Cores 22/23; (b) Cores 24/25

Figure 3.7 Delamination observed in Core 24

### 3.4 Texas Overlay Test (OT)

Texas Overlay Tests were conducted on the top and bottom sections of Cores 5 and 6 extracted from the I-35 section. Table 3.3 presents the results showing very poor resistance to cracking. The top specimens were collected from the top 0 to 1.5 inches of the extracted cores while the bottom specimens were taken from a depth of 1.5 to 3 inches from the surface. Figure 3.8 (a) and (b) show photographic views of the specimens before and after test. A very dry mix

condition was observed during testing. Generally, an asphalt mix with more than 300 cycles is expected to exhibit satisfactory resistance to fatigue cracking in the field. Based on these results, the resistance to fatigue cracking of the tested specimens was extremely low.

Table 3.3 Results of the Texas Overlay test

| Core (Depth from Surface) | Cycles to failure |
|---|---|
| 5 top (0 to 1.5 inch) | 6 |
| 5 bottom (1.5 to 3 inch) | 6 |
| 6 top (0 to 1.5 inch) | 4 |
| 6 bottom (1.5 to 3 inch) | 6 |

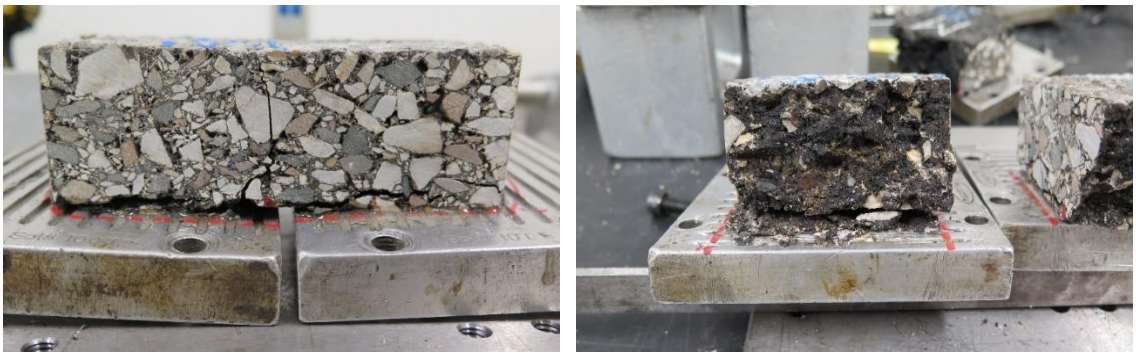

(a) (b)

Figure 3.8 Samples (a) before and (b) after Texas Overlay Test

### 3.5 Tensile Strength Ratio (TSR) and Indirect Tensile Asphalt Cracking Test (IDEAL-CT)

The TSR tests were conducted on five (5) cores extracted from the I-35 section. Three (3) of these cores were used as the control subset and the remaining two (2) cores were used as the preconditioned subset. The tests were conducted in accordance with the AASHTO T 283 [11] method. Table 3.4 summarizes the results obtained for each subset. A very low TSR value was observed (0.57). Also, low indirect tensile strength values were observed for all subsets. Cracked or broken aggregates were observed in all subsets. A high moisture-induced damage was observed in the preconditioned subset.

The load-displacement curves obtained for the cores from the TSR tests were further analyzed to determine the Cracking Tolerance index (CT index) using the principle of the IDEAL-CT test following the NCHRP 20-30/IDEA 195 method [12]. From these analyses, the

tested cores exhibited CT indices of below 80, indicating a weak resistance to fatigue. Nevertheless, higher CT indices were observed for pre-condition samples. The CT index for Core 4 could not be determined, because of difficulties encountered in measuring pertinent displacements. Table 3.4 summarizes the results of the CT indices, and Figure 3.9 shows the load vs displacement curves for the tested cores.

Table 3.4 Results of the TSR and CT indices for the tested cores

| **Core Number** | **4** | **8** | **14** | **7** | **15** |
|---|---|---|---|---|---|
| **Control or Pre-conditioned?** | C | C | C | P | P |
| **Load, lbf** | 1150 | 1334 | 1414 | 955 | 627 |
| **IDEAL CT Index (Min. 80)** | NA | 8 | 9 | 14 | 66 |
| **Indirect Tensile Strength, psi** | 55 | 59 | 64 | 41 | 27 |
| **Average Control and Pre-Con, psi** | 59 | | | 34 | |
| **Tensile Strength Ratio (min 0.8/0.75 design/field)** | 0.57 | | | | |

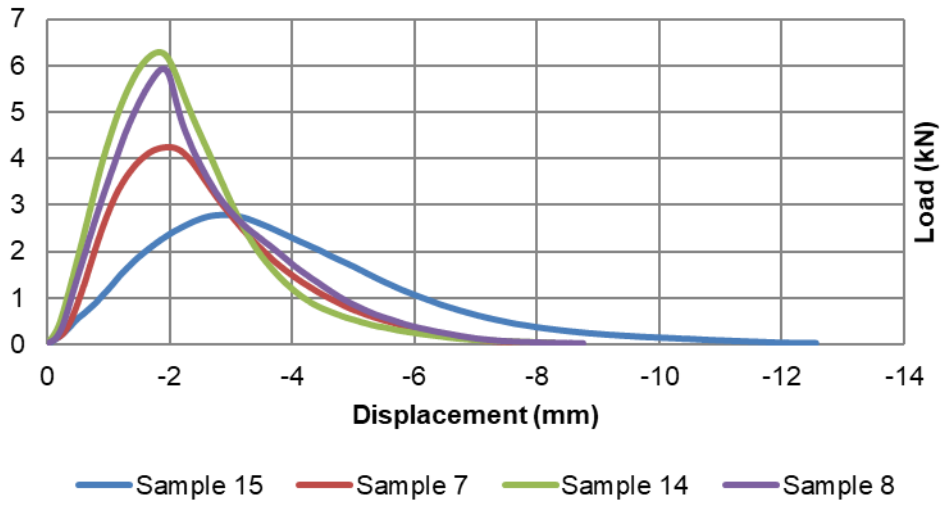


Figure 3.9 Load vs displacement curves of the tested cores

# 4. SUBSURFACE INVESTIGATION AND TRAFFIC SPEED DEFLECTION DEVICE (TSDD)

As noted earlier, a Traffic Speed Deflection Device (TSDD) survey was conducted in 2020 as part of a pooled fund study, participated by ODOT, on the same sections of I-35 and SH-7 used in this study. Access to the TSDD data to the OU team was provided by the Pavement Management group at ODOT. As noted previously, the deflection values from the TSDD data were compared selectively with the FFWD data from this Task Order. These comparisons are presented in this section along with some correlations between the two sets of data (TSDD and FFWD).

A Hawkeye software pass was provided by ODOT to compile and analyze the TSDD results. The Hawkeye software reports deflections, roughness, rut depths, texture, distresses, and geometric properties. Of these, only deflection values were compared in this Task Order. Other comparisons and correlations can be done in future studies. In TSDD, load-induced deflection data are collected using Doppler lasers, while the instrumented vehicle travels at the traffic speed (Figure 4.1). The TSDD system is equipped with image, geoposition, length measurement, straightedge and laser systems that are capable of collecting and recording these data. TSDD is capable to measuring these parameters for both wheels. Measurements at traffic speed eliminates traffic control needs. Several state DOTs are considering the TSDD technology for network-level pavement management.

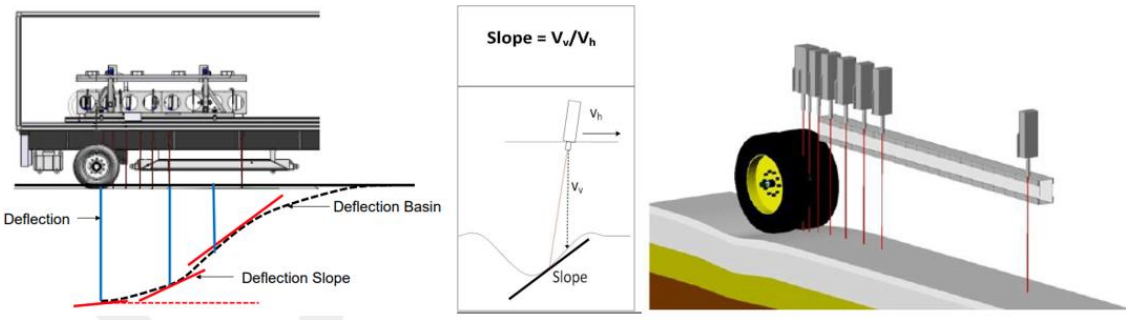


Figure 4.1 Deflection measurement using Traffic Speed Deflection Device (TSDD)

Table 4.1 describes the mean, standard deviation, and minimum and maximum values for all sections. Slightly higher rut, deflections and roughness values were observed on the east-bound lane of SH-7 compared to the west-bound lane. No significant differences were observed between the two sections (north and south of SH-7) of I-35. However, a higher mean deflection was observed on both north- and south-bound lanes located north of SH-7.

Table 4.1 Summary of deflection, rut depths and roughness results

| Segment | Measure | Mean | Standard Deviation | Maximum | Minimum |
|---|---|---|---|---|---|
| **SH-7 East-bound** | D0 (mils) | 3.47 | 1.30 | 9.20 | 0.00 |
| | Rut (in) | 0.26 | 0.08 | 0.49 | 0.05 |
| | IRI (in/mi) | 69.48 | 34.56 | 278.00 | 22.00 |
| **SH-7 West-bound** | D0 (mils) | 3.26 | 1.61 | 10.60 | 0.00 |
| | Rut (in) | 0.21 | 0.07 | 0.48 | 0.06 |
| | IRI (in/mi) | 56.00 | 28.65 | 291.00 | 20.00 |
| **I-35 (north of SH-7) North-bound** | D0 (mils) | 0.91 | 1.46 | 9.00 | 0.00 |
| | Rut (in) | 0.13 | 0.06 | 0.43 | 0.03 |
| | IRI (in/mi) | 63.88 | 47.33 | 527.00 | 21.00 |
| **I-35 (north of SH-7) South-bound** | D0 (mils) | 1.17 | 1.48 | 11.20 | 0.00 |
| | Rut (in) | 0.10 | 0.05 | 0.36 | 0.04 |
| | IRI (in/mi) | 59.48 | 41.44 | 359.00 | 20.00 |
| **I-35 (south of SH-7) North-bound** | D0 (mils) | 0.41 | 1.16 | 12.20 | 0.00 |
| | Rut (in) | 0.14 | 0.06 | 0.45 | 0.03 |
| | IRI (in/mi) | 70.67 | 39.48 | 465.00 | 30.00 |
| **I-35 (south of SH-7) South-bound** | D0 (mils) | 0.51 | 1.43 | 19.60 | 0.00 |
| | Rut (in) | 0.08 | 0.04 | 0.49 | 0.03 |
| | IRI (in/mi) | 52.95 | 51.23 | 526.00 | 22.00 |

### 4.1 TSDD and FFWD Correlations

Deflections from the TSDD survey were compared with the corresponding deflections from the FFWD testing on both I-35 and SH-7 sections. One of the major challenges involved in this comparison was to match locations where the deflection measurements were taken by each device. Global Positioning System (GPS) data were used to identify identical (or nearly identical) locations for each (FFWD and TSDD).

Figures 4.2, 4.3, 4.4 and 4.5 show a comparison between normalized deflections under the center of the load for TSDD (D0) and FFWD (W1) for both SH-7 and I-35 sections. The deflection values from both measurements (FFWD and TSDD) were correlated for each direction of SH-7 and I-35 sections. The corresponding $R^2$ values were 0.34, 0.55, 0.47 and 0.26 for the east-bound SH-7, west-bound SH-7, north-bound I-35, and south-bound I-35, respectively. As mentioned previously, several deflection points were not recorded/reported by TSDD. So, deflection values at these locations could not be compared. From Figures 4.4 and 4.5 on I-35, there are some gaps between points. Figure 4.6 shows the relationships between

W1 and D0 for all data combined. A correlation of 0.45 and a coefficient of determination ($R^2$) of 0.21 were observed. Overall, these results indicate a need for exploring these data further. As noted in the recommendations, having both TSDD and FFWD data (along with GPR data) is a rare opportunity for local calibration of coefficients used by TSDD in assessing pavement conditions and remaining service life.

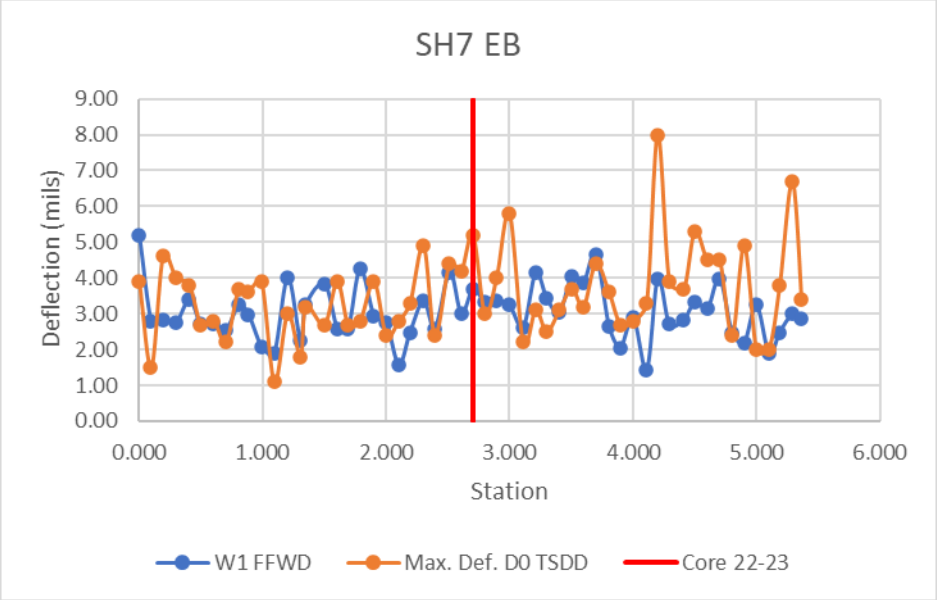


Figure 4.2 TSDD and FFWD deflections for east-bound SH-7

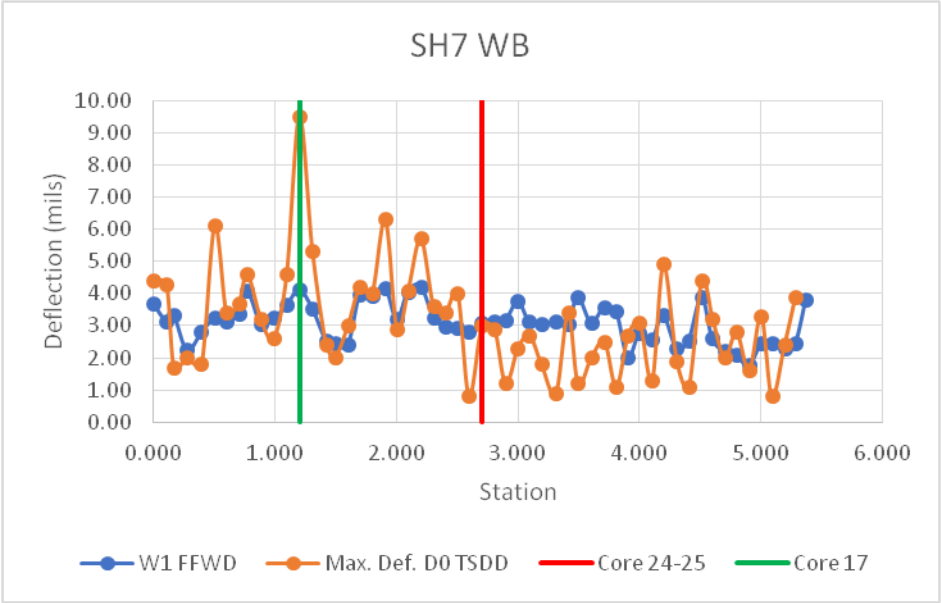


Figure 4.3 TSDD and FFWD deflections for west-bound SH-7

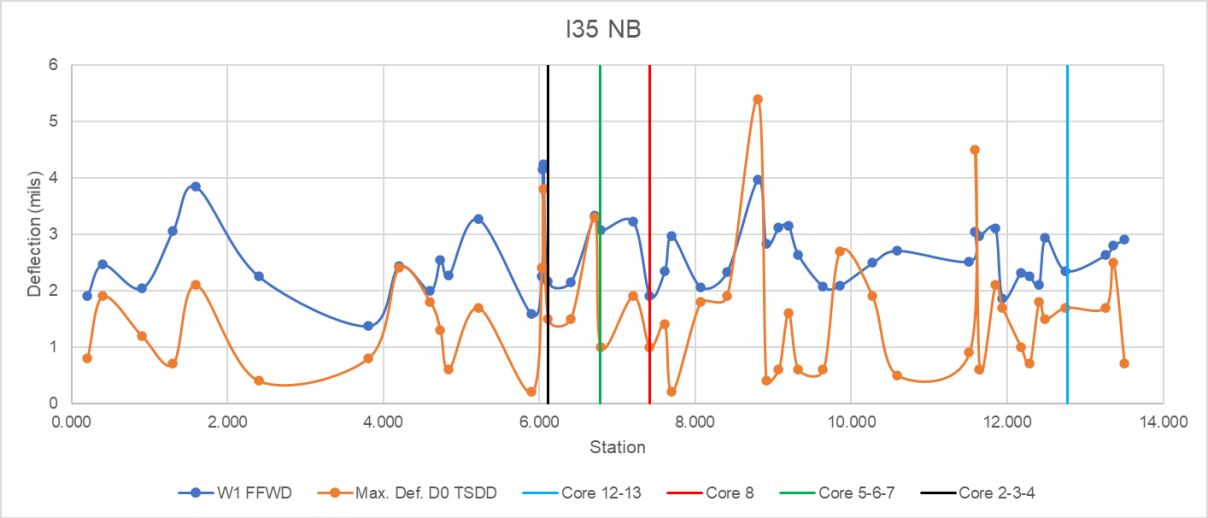


Figure 4.4 TSDD and FFWD deflections for north-bound I-35

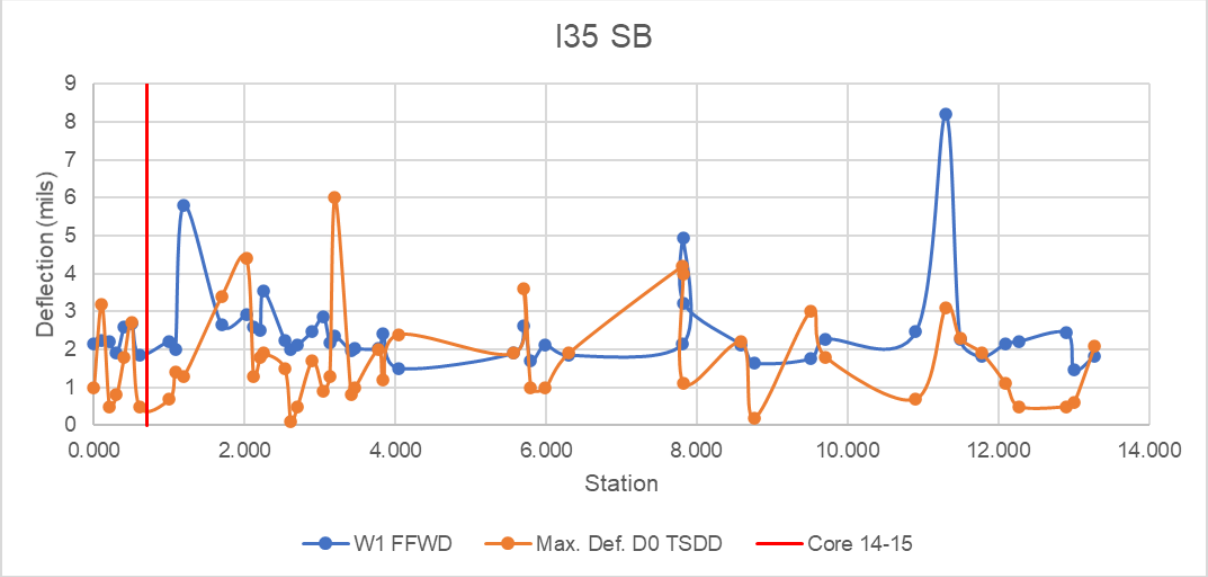


Figure 4.5 TSDD and FFWD deflections for south-bound I-35

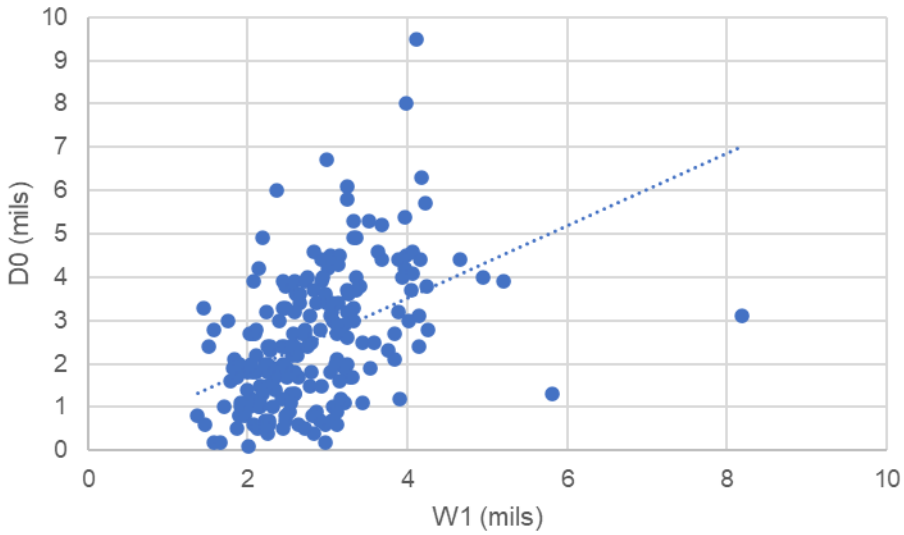


Figure 4.6 Relationship between TSDD and FFWD deflections

## 5. REHABILITATION OPTIONS AND COST ANALYSIS

Based on the results obtained from the field survey, laboratory tests and TSDD results presented in the preceding sections and findings from ODOT Task Order 2160-18-09, the following repair options were evaluated for the rehabilitation of the studied sections of SH-7 and I-35. The FHWA suggests the following life cycle cost analysis (LCCA) procedures when evaluating design alternatives [14]:

1. Establish design alternatives [and AP]
2. Determine [performance period and] activity timing
3. Estimate costs [agency and user]
4. Compute [net present value] life cycle costs
5. Analyze results
6. Reevaluate design strategies

Equivalent Uniform Annual Cost (EUAC) is an alternative LCCA method that has been used widely in transportation decision making when service lives differ in length for given alternatives [15]. In the calculation methodology, all incurred costs expected throughout the service life of an alternative are brought to a base year, summed, and then annualized

according to the treatment's service life as determined by field data and pavement manager's professional judgment. The EUAC equation can be expressed follows:

$$\mathbf{EUAC\ (i\%) = [\Sigma P] * [i(1+i)^n \div (1+i)^n - 1)]}$$

where:

i = discount rate (in this case, 4% as suggested in literature for highway projects)

P = present value

n = pavement treatment *anticipated service life*

The *per-lane-mile (12 feet wide considered here)* repair scenarios are shown in the following tables for the various locations. Routine interim maintenance (e.g., crack sealing) and user costs were not considered in the analysis. Also, cost of tack coats was not considered.

The LCCA results for the repair options for the I-35 section are shown in Table 5.1. Based upon the input data (treatment type, expected service life and total initial cost), Option 2 yields the lowest EUAC ($11,381) than the other options given its lower initial cost and relatively long service life. Option 4 yields the highest estimated life cycle cost ($26,931).

Table 5.1 LCCA estimations: north-bound I-35, north of Mile Post 52, outside lane repair options

| ID | Repair | Cost | Life (years) | LCCA (EUAC) | LCCA Rank (lowest EUAC = 1) |
|---|---|---|---|---|---|
| 1 | 1-in. Cold Milling Pavement, 2-in. SMA (PG 64E-28), 1-in. CAM (PG 64E-28) | $147,696 | 13 | $14,791 | 2 |
| 2 | 1-in. Cold Milling Pavement, 1.25-in. BX (PG 64E-28), 1-in. CAM (PG 64E-28) | $106,808 | 12 | $11,381 | 1 |
| 3 | 1-in. Cold Milling Pavement, 1.25-in. PFC, 1-in. CAM (PG 64E-28) | $117,910 | 8 | $17,513 | 3 |
| 4 | 4-in. Cold Milling Pavement, 1.5-in. S5 (PG 76E-28), 2.5-in. S3 (PG 76E-28), 1.5-in. RIL (PG 76E-28) | $268,928 | 13 | $26,931 | 4 |

The FHWA suggests that a sensitivity analysis be included in LCCA (Step 5 – Analyze Results) to provide a greater insight into the uncertainty that exists within the analyses. The sensitivity analysis will help determine the effect of different assumptions on the output (rankings). The Option 2 (lowest EUAC) scenario shown in the preceding table would have to be calculated with a 9-year service life (EUAC = $14,365) to make it comparable to the nearest

EUAC option (Option 1). For the given cost, the service life of Option 4 would need to be at least 24 years to yield an EUAC of $17,638 and be comparable to the third-ranked option (Option 3). The sensitivity analysis provides the evaluator with an indication about how sensitive the output is to the selected service life to inform decision making.

The LCCA results for the overlay scenario for the I-35 section are shown in Table 5.2. Option 2 (1.25-in. BX) yields the lowest EUAC at $5,397, followed by Option 4 (S5 mix), consistent with their relatively lower initial costs and similar service lives. Options 1 (SMA) and 3 (PFC) have comparable EUACs (~$9,170) and have the highest estimated life cycle costs of these alternatives for the given data.

Table 5.2 LCCA estimations: I-35 overlay repair options

| ID | Repair | Cost | Life (years) | LCCA (EUAC) | LCCA Rank (lowest EUAC = 1) |
|---|---|---|---|---|---|
| 1 | 2-in. SMA (PG 64E-28) | $91,524 | 13 | $9,166 | 3 |
| 2 | 1.25-in. BX (PG 64E-28) | $50,656 | 12 | $5,397 | 1 |
| 3 | 1.25-in. PFC (PG 64E-28) | $61,739 | 8 | $9,170 | 3 |
| 4 | 1.5-in. S5 (PG 64E-28) | $61,121 | 12 | $6,513 | 2 |

The sensitivity analysis shows that Option 2 would need to be calculated with a 10-year service life to yield a comparable EUAC ($6,245) to Option 4 given the stated costs. The service life for Option 1 would need to be at least 20 years to yield an EUAC of $6,734 and be comparable to the second ranked option (Option 4), while Option 3 would require a 12-year service life (EUAC $6,578) to be comparable to second-ranked Option 4.

The LCCA results for the repair options for the east-bound lane of SH-7 are shown in Table 5.3. Given the similarities in initial costs and expected service lives, the calculated EUACs for both options are comparable.

Table 5.3 LCCA estimations: EB SH-7 inside lane, repair options

| ID | Repair | Cost | Life (years) | LCCA (EUAC) | LCCA Rank (lowest EUAC = 1) |
|---|---|---|---|---|---|
| 1 | 2-in. Cold Milling Pavement, 2-in. SMA (P G64E-28) | $107,364 | 13 | $10,752 | similar |
| 2 | 2-in. Cold Milling Pavement, 2-in. S4 (PG 64E-28) | $98,861 | 12 | $10,534 | similar |

The LCCA results for the overlay scenario for SH-7 are shown in Table 5.4. Option 3 (0.75-in. UTBWC-Type C) yields the lowest EUAC at $4,617, followed by Options 1 and 4 (BX and S5 mix, respectively). Options 2 (PFC) and 5 (SMA) have comparable EUACs (~$9,170) and have the highest estimated life cycle costs of these alternatives for the given input data.

Table 5.4 LCCA estimations: SH-7 overlay repair options

| ID | Repair | Cost | Life (years) | LCCA (EUAC) | LCCA Rank (lowest EUAC = 1) |
|---|---|---|---|---|---|
| 1 | 1.25-in. BX (PG 64E-28) | $50,656 | 12 | $5,397 | 2 |
| 2 | 1.25-in. PFC (PG 64E-28) | $61,738 | 8 | $9,170 | 4 |
| 3 | 0.75-in. UTBWC (Type C) | $31,089 | 8 | $4,617 | 1 |
| 4 | 1.5-in. S5 (PG 64E-28) | $61,121 | 12 | $6,513 | 3 |
| 5 | 2-in. SMA (PG 64E-28) | $91,524 | 13 | $9,166 | 4 |

The sensitivity analysis shows that the lowest cost option (Option 3) would need to be calculated with a 7-year service life to yield a similar EUAC ($5,180) to the second-ranked Option 1 given the stated costs.

The LCCA results reported herein should be evaluated in accordance with FHWA “good practices” (Step 6) and agency experience and practice. Generally, LCCA results are coupled with other decision-support factors such as “risk, available budgets, and political and environmental concerns” (FHWA 2002). The output from an LCCA should not be considered the answer, but merely an indication of the cost effectiveness of alternatives (FHWA 2002).

## 6. CONCLUSIONS AND RECOMMENDATIONS

The main objective of this Task Order was to perform a subsurface investigation using the specialized GPR system with capability to take continuous video for identifying locations of subsurface distresses and making data-driven recommendations for maintenance and rehabilitation. In this Task Order, field data from GPR and FFWD were combined with laboratory performance test (SCB, IDEAL-CT, TSR, HWT, OT) data for both I-35 and SH-7 sections and the results were used to identify the causes of the distresses observed. Also, deflection data from the FFWD tests were compared and correlated selectively with the TSDD data collected as

part of a pooled fund study, participated by ODOT. The overall findings of this Task Order are listed below:

2. The GPR images showed two different types of pavements in the studied section of I-35. It was observed that the north of Mile Post 51.5 has Jointed Concrete Pavement (JCP) while the section south of Mile Post 51.5 has Continuously Reinforced Concrete Pavement (CRCP). The JCP section showed severe reflective cracking. The main distresses observed on the CRCP section were longitudinal edge cracking and edge failure. The presence of joint between the shoulder and lane inside the stripe paint is expected to be the main cause of longitudinal edge failure.
3. Significant rutting, cracking and longitudinal joint cracking were observed on the east-bound lane of SH-7. The GPR images and extracted cores revealed a very thick layer of HMA in this section. A loose or delaminated fabric layer not attached to the pavement below might be responsible for causing shear failure and rutting in the HMA layer. The GPR data exhibited an increase in moisture over the joint indicating infiltration of water through the longitudinal joint crack. The inside lanes of SH-7 were observed to be in fairly good conditions.
4. The elastic modulus (E) values of the surface and subgrade layers of I-35 and SH-7 sections were determined using the FFWD tests. Overall, good modulus (E) values were observed for the I-35 section and low modulus values were observed for the east-bound inside lane of SH-7, where major depressions and ruts were observed.
5. Laboratory performance tests, namely I-FIT (SCB), IDEAL-CT, OT and TSR tests were conducted on extracted cores from the I-35 section. The Flexibility Index (FI) from I-FIT test and CT Index from the IDEAL-CT test did not meet the minimum passing criteria for fatigue cracking. Also, very low cycles to failure were observed from the OT test. The results indicated the presence of a very dry mix on the I-35 section that is likely prone to additional fatigue cracking without appropriate rehabilitation measures.
6. The HWT tests were conducted on cores collected from the east-bound and west-bound lanes of the SH-7 section. The results of the HWT tests indicated potential for rut failure of the SH-7 section. The Core 24, which was severely delaminated and located next to the longitudinal joint, was severely damaged during the HWT test. Also, the TSDD data exhibited higher rut and roughness for the east-bound lane of SH-7.

7. The FFWD and TSDD deflection data under the center of the loads exhibited a correlation of 0.45. The overall $R^2$ between the FFWD and TSDD deflection values for both sections were found as 0.21. A stronger correlation was observed for the west-bound lane of SH-7.
8. Based on the LCCA analysis, the recommended repair/rehabilitation options, from least costly to most costly, were found as follows:
    a. North-bound I-35, north of Mile Post 51.5, outside lane
        i. Cold mill up to 1-in. of the existing pavement and replace with 1.25-in. of BX (PG 64E-28) and 1-in of Crack Attenuating Mix (CAM) (PG 64-28)
    b. I-35 overlay
        i. Place 1.25-in. of BX (PG 64E-28) on top of the existing pavement
    c. East-bound SH-7 inside lane repair options are similar to those recommended in ODOT Task Order 2160-18-09.
        i. Cold mill up to 2-in. of existing pavement and replace with 2-in. of Stone Matrix Asphalt (SMA) (PG 64E-28), or
        ii. Cold mill up to 2-in. of the existing pavement and replace with 2-in. of S4 (PG 64E-28)
    d. SH-7 overlay
        i. Place 0.75-in. of Ultra-Thin Bonded Wearing Course (UTBWC) Type C, or
        ii. Place 1.25-in. of BX (PG 64E-28) on top of the existing section
9. The asphalt mixes should be designed using a Balanced Mix Design (BMD) approach, when possible. The Stone Matrix (SMA) is a standard mix choice for BMD. The BX mix is similar to TOM-C (Thin Overlay Mix Type C) used by Texas DOT. A Special Provision for the BX mix was developed as a part of an ongoing ODOT Task Order (Task Order# 2160-231-05). A BMD Special Provision for the BX mix was also developed for the same Task Order. The following should be considered during project letting and construction:
    a. CAM Special Provision and BAMS pay item will need to be created should it be specified in project plans.
    b. Non-tracking tack coat is recommended between lifts/layers of asphalt mix.
10. In order to address specific issues of pavements, other conventional/unconventional mixes could be considered as overlay. For example: a Permeable Friction Coarse (PFC) mix can be considered to address drainage issues like hydroplaning and

rooster-tail effects. However, no structural value is typically assigned to a PFC layer. It is a sacrificial mix that generally has lower life than a dense graded mix.

11. Specialized GPR used in this project, in collaboration with TTI/TAMU, collected data at highway speed. This can be a useful tool for selective data-driven coring of pavement, which is a destructive process.
12. FFWD or FWD when used in conjunction with TSDD can be a useful tool for validating TSDD results and identifying pavement conditions (project level) confidently. Also, using pavement layer thicknesses from the GPR data at highway speed enhances the utility of TSDD data for network-level application.

## REFERENCES


[1] Katicha, S., Shrestha, S., Flintsch, G., and Diefendender, B. (2020). “Network Level Pavement Structural Testing with the Traffic Speed Deflectometer”, Project 111810, Report VTRC 21-R4, Virginia Department of Transportation (VDOT)

[2] Rada, G.R., Nazarian, S., Visintine, B.A., Siddharthan, R.V., & Thyagarajan, S. (2016). Pavement Structural Evaluation at the Network Level: Final Report.

[3] Triplow, C., and Wix, R. (2017). “An Evaluation of Traffic Speed Deflectometer for Main Roads Western Australia”. Australian Road Research Board

[4] Flintsch, G.W., Ferne, B., Diefenderfer, B.K., & Katicha, S.W. (2012). Evaluation of Traffic Speed Continuous Deflection Devices.

[5] Katicha, S., Flintsch, G., Shrestha, S., and Thyagarajan, S. (2017). Demonstration of Network Level Pavement Structural Evaluation with Traffic Speed Deflectometer: Final Report, Transportation Pooled Fund Program, TPF 5(282), https://www.pooledfund.org/Details/Study/518.

[6] GeoSolve LTD. (2016). “Traffic Speed Deflectometer, The Application of TSD Data in New Zealand for Asset Management and Design”, Ref. 150003, New Zealand Transport Agency.

[7] AASHTO T 209 (2012). “Standard Method of Test for Theoretical Maximum Specific Gravity (Gmm) and Density of Hot-Mix Asphalt (HMA).” American Association of State and Highway Transportation Officials.

[8] OHD L-14 (2018). “ODOT Standard Method of Test for Bulk Specific Gravity, Percent Density, and Longitudinal Joint Density of Compacted Asphalt Mixtures”. Oklahoma Department of Transportation.

[9] OHD L-55 (2014). “ODOT Standard Method of Test for Hamburg Rut Testing of Compacted Hot-Mix Asphalt (HMA)”. Oklahoma Department of Transportation.

[10] AASHTO TP 124 (2018). “Standard Method of Test for Determining the Fracture Potential of Asphalt Mixtures Using the Flexibility Index Test (FIT).” American Association of State and Highway Transportation Officials.

[11] AASHTO T 283 (2018). “Standard Method of Test for Resistance of Compacted Asphalt Mixtures to Moisture-Induced Damage.” American Association of State and Highway Transportation Officials.

[12] Zhou, F. (2019). Development of an IDEAL Cracking Test for Asphalt Mix Design, Quality Control and Quality Assurance. NCHRP-IDEA Program Project Final Report, (195).

[13] TxDOT Tex-248-F (2019). “Test Procedure for Overlay Test.” Texas Department of Transportation.

[14] FHWA (2002).” Life-Cycle Cost Analysis Primer”. Federal Highway Administration.

[15] Sinha, K. C., & Labi, S. (2011). “Transportation decision making: Principles of project evaluation and programming”. John Wiley & Sons.

# APPENDIX A: DETAILS AND PHOTOGRAPHS OF CORES

| Cores I-35 | Lattitude | Longitude | Dir. | Top Lift (mm) | HMA (mm) | Base (mm) | Total (mm) | Top Lift (in.) | HMA (in.) | Base (in.) | Total (in.) | Core Notes (mm) |
|---|---|---|---|---|---|---|---|---|---|---|---|---|
| Staging Area | 34.33316 | -97.15114 | NB | | | | | | | | | |
| Begin | 34.37638 | -97.14418 | NB | | | | | | | | | |
| 2 | 34.46068 | -97.14470 | NB | 15 | 177 | | 177 | 0.59 | 6.97 | | 6.97 | Mid. Lane. |
| 3 | 34.46068 | -97.14470 | NB | 14 | 177 | | 177 | 0.55 | 6.97 | | 6.97 | 2' S. of core 2. |
| 4 | 34.46068 | -97.14470 | NB | 17 | 535 | 310 | 535 | 0.67 | 21.06 | 12.20 | 21.06 | Over shoulder line. 125 del, 180 lt. strip, 415 del. BBFAT |
| 5 | 34.46884 | -97.15230 | NB | 37 | 117 | | | 1.46 | 4.61 | | | Mid. Lane. Thick tack 35. Fabric 117. |
| 6 | 34.46884 | -97.15230 | NB | 45 | 172 | | | 1.77 | 6.77 | | | 2' S. of core 2. Fab. 45 and fabric 119. |
| 7 | 34.46884 | -97.15230 | NB | 40 | 224 | 286 | 510 | 1.57 | 8.82 | 11.26 | 20.08 | Mid. Shoulder. Del. 185. |
| 8 | 34.47726 | -97.15656 | NB | 45 | 150 | | | 1.77 | 5.91 | | | 1' left of shoulder line. Thick tack 45 and 135. |
| 12 | 34.55026 | -97.19055 | NB | 40 | 255 | 249 | 504 | 1.57 | 10.04 | 9.80 | 19.84 | Mid. Lane over crack filled crack. Crack to 40. Thick tack 40 and 130. Del. 255. |
| 13 | 34.55026 | -97.19055 | NB | 60 | 282 | 223 | 505 | 2.36 | 11.10 | 8.78 | 19.88 | 2' right of shoulder line. Cracked to 60. Del. 176. 230 minor stripping. |
| 14 | 34.55026 | -97.19055 | SB | 25 | 163 | | | 0.98 | 6.42 | | | RW (right wheel path). |
| 15 | 34.55026 | -97.19055 | SB | 30 | 194 | 296 | 485 | 1.18 | 7.64 | 11.65 | 19.09 | Shoulder line. Slight strip 30 and 70. Del. 153 and 355. 355 to 450 fully cracked. |
| End | 34.55987 | -97.19314 | | | | | | | | | | |

| Cores SH-7 | Lattitude | Longitude | Dir. | Top Lift (mm) | HMA (mm) | Base (mm) | Total (mm) | Top Lift (in.) | HMA (in.) | Base (in.) | Total (in.) | Core Notes (mm) |
|---|---|---|---|---|---|---|---|---|---|---|---|---|
| Staging Area | 34.50669 | -97.17723 | WB | | | | | | | | | |
| Begin | 34.51004 | -97.19488 | WB | | | | | | | | | |
| 17 | 34.52051 | -97.21273 | WB | 25 | 447 | | 447 | 0.98 | 17.60 | | 17.60 | RW thru crack. Cracked to Fab. 25. |
| 22 | 34.52131 | -97.23798 | EB | 32 | 390 | 35 | 425 | 1.26 | 15.35 | 1.38 | 16.73 | RW. Fab. 32. Del. 225. |
| 23 | 34.52131 | -97.23798 | EB | 25 | 410 | 95 | 505 | 0.98 | 16.14 | 3.74 | 19.88 | LW near CL in rutted area. Fab. 25. Some strip to 40. Del. 235. **Stripping in core hole from 50 to 100. |
| 24 | 34.52131 | -97.23798 | WB | 32 | 440 | 80 | 520 | 1.26 | 17.32 | 3.15 | 20.47 | LW over crack. Fab. 32. Del. and some strip at 75 and 260. |
| 25 | 34.52131 | -97.23798 | WB | 33 | 435 | 70 | 505 | 1.30 | 17.13 | 2.76 | 19.88 | RW. Fab. 33. Del. 67 and 345. |
| End | 34.52134 | -97.28487 | | | | | | | | | | |


Figure A.1 Core #2 on I-35


Figure A.2 Core #3 on I-35


Figure A.3 Core #4 on I-35


Figure A.4 Core #5 on I-35

Figure A.5 Core #6 on I-35

Figure A.6 Core #7 on I-35

Figure A.7 Core #8 on I-35

Figure A.8 Core #12 on I-35

Figure A.9 Core #13 on I-35

Figure A.10 Core #14 on I-35


Figure A.11 Core #15 on I-35


Figure A.12 Core #17 on SH-7


Figure A.13 Core #22 on SH-7


Figure A.14 Core #23 on SH-7


Figure A.15 Core #24 on SH-7


Figure A.16 Core #25 on SH-7

# APPENDIX B: GRAPHICAL REPRESENTATION OF GROUND PENETRATING RADAR DATA


Figure B.1 Raw GPR data for a 1-mile (approximately) section of north-bound I-35

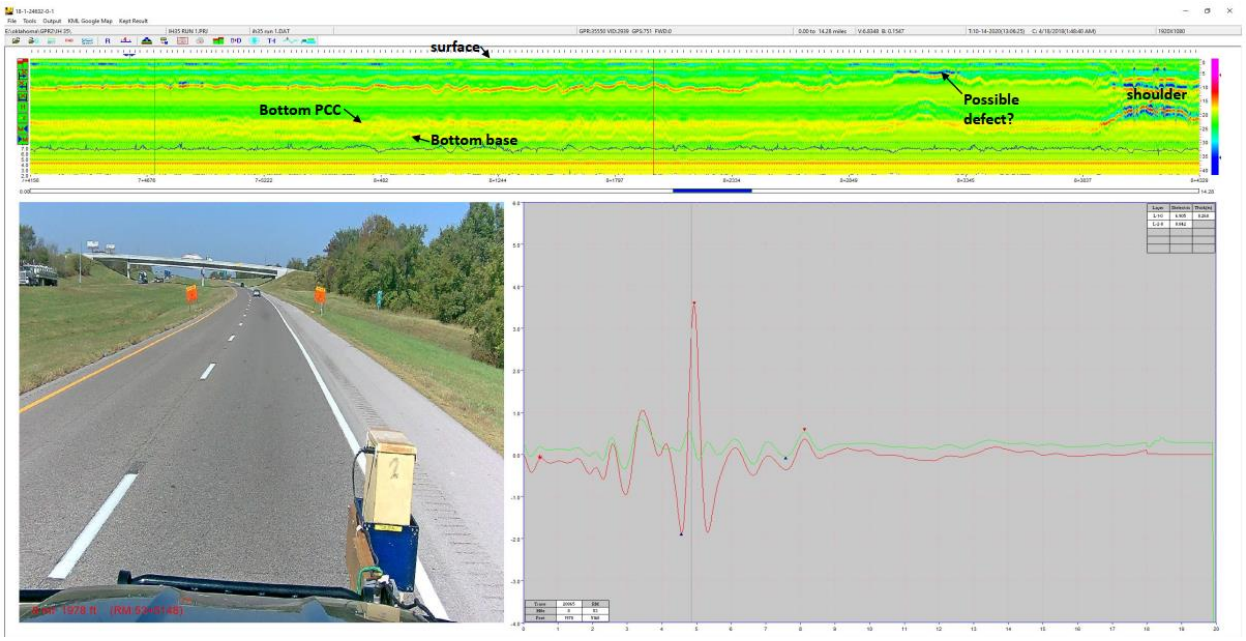


Figure B.2 Removing the surface to highlight subsurface information of I-35

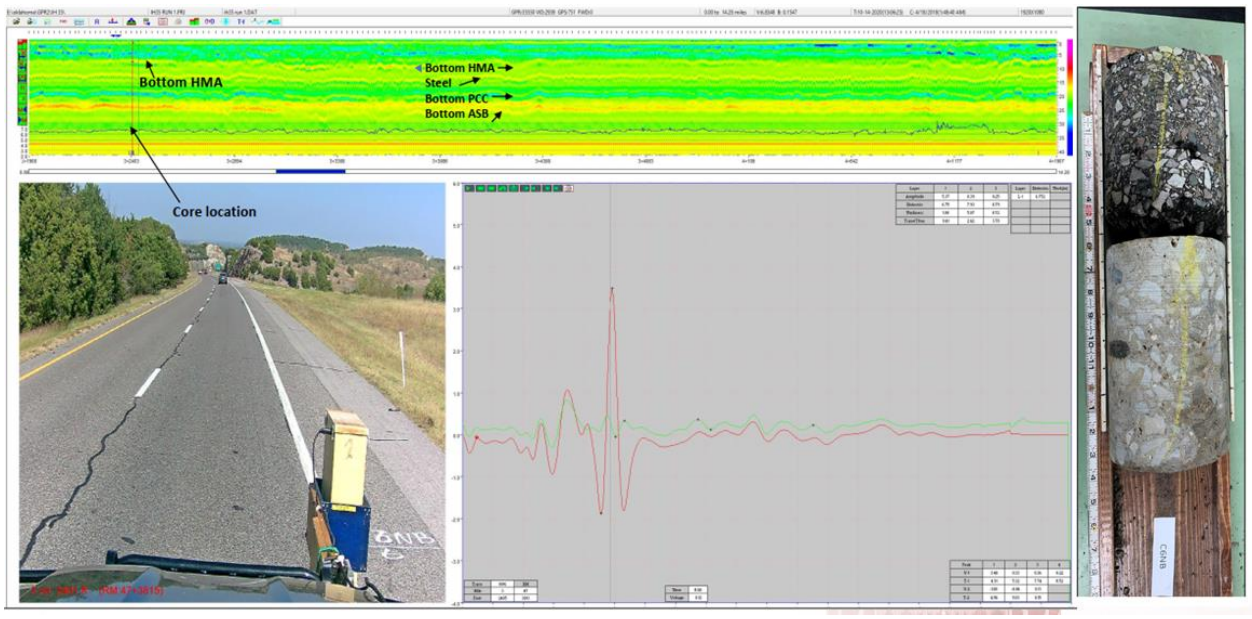


Figure B.3 Location of Core 6 from ODOT survey on I-35


Figure B.4 Inside lane at transition from CRCP to JCP @ Mile Post 51.5 on I-35

RM 58.6 looks like concrete shoulder

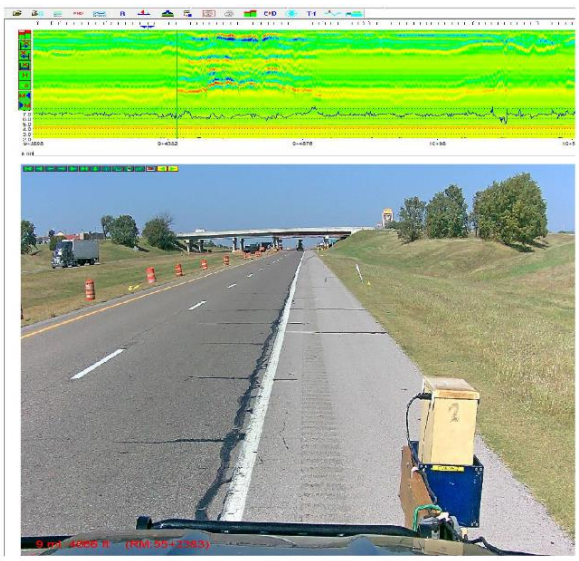

RM 55.4 looks like Flexible shoulder (joint inside white line)

Figure B.5 GPR on shoulders (Mile Post 58.6 and 55.4) of I-35

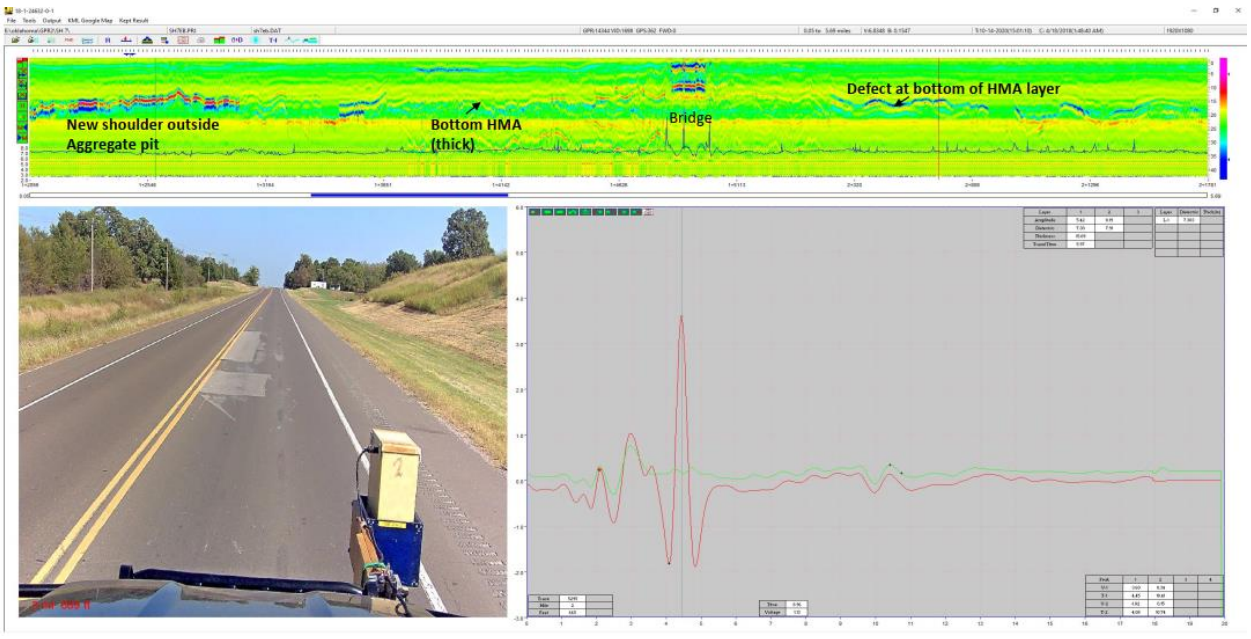


Figure B.6 GPR on west-bound lane of SH-7

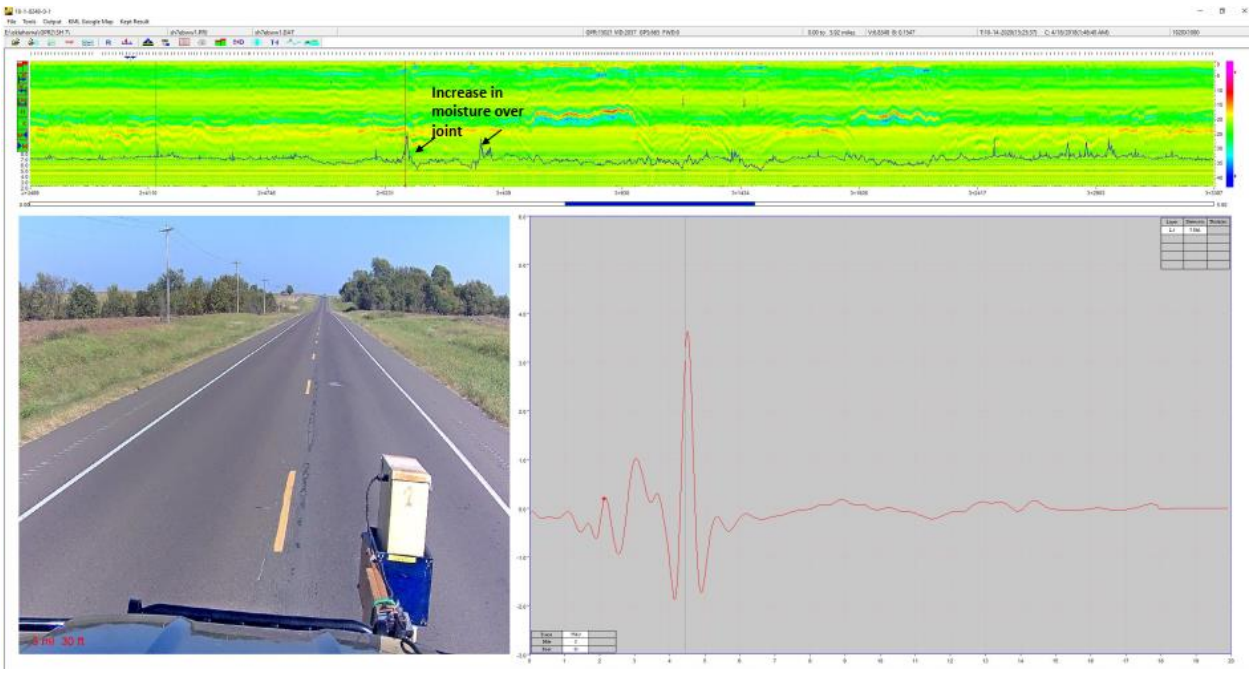


Figure B.7 GPR over rutted section on east-bound SH-7